



1

2

3 **Coordination of rooting, xylem, and stomatal strategies explains the response of conifer**  
4 **forest stands to multi-year drought in the Southern Sierra Nevada of California**

5

6 Junyan Ding<sup>1,2</sup>, Polly Buotte<sup>3</sup>, Roger Bales<sup>4</sup>, Bradley Christoffersen<sup>5</sup>, Rosie A. Fisher<sup>6,7</sup>, Michael  
7 Goulden<sup>8</sup>, Ryan Knox<sup>1</sup>, Lara Kueppers<sup>1,3</sup>, Jacquelyn Shuman<sup>6</sup>, Chonggang Xu<sup>9</sup>, Charles D.  
8 Koven<sup>1</sup>

9 1. Climate and Ecosystem Sciences Division, Lawrence Berkeley National Lab, Berkeley,  
10 USA

11 2. Pacific Northwest National Lab, Richland, WA, USA

12 3. Energy and Resources Group, University of California, Berkeley, USA

13 4. Sierra Nevada Research Institute, University of California, Merced, USA

14 5. Department of Biology, University of Texas, Rio Grande Valley, USA

15 6. Climate and Global Dynamics Division, National Center for Atmospheric Research,  
16 Bold, USA

17 7. Laboratoire Évolution & Diversité Biologique, CNRS:UMR 5174, Université Paul  
18 Sabatier, Toulouse, France

19 8. Dept. of Earth System Science, University of California, Irvine, USA

20 9. Earth and Environmental Sciences Division, Los Alamos National Laboratory, Santa Fe,  
21 New Mexico, USA

22 Corresponding author: Junyan Ding (junyan.ding@pnnl.gov)

23 **Key Points:**

- 24 • We perform a sensitivity analysis using the model FATES-Hydro to explore the co-  
25 ordination of leaf, xylem, and root hydraulic traits of pine in Southern Sierra Nevada.
- 26 • We find that rooting depth is the major control on water and carbon fluxes, and that deep-  
27 rooted pines with risky stomata have the highest GPP but also the highest drought  
28 mortality risk.
- 29 • Resolving both the plant water sourcing strategies and subsurface processes are critical to  
30 represent drought impacts on conifer forests.
- 31



32

### Abstract

33 Extreme droughts are a major determinant of ecosystem disturbance, which impact plant  
34 communities and feed back to climate change through changes in plant functioning. However,  
35 the complex relationships between above- and belowground plant hydraulic traits, and their  
36 role in governing plant responses to drought, are not fully understood. In this study, we use a  
37 plant hydraulics model, FATES-Hydro, to investigate ecosystem responses to the 2012-2015  
38 California drought, in comparison with observations, for a site in the southern Sierra Nevada  
39 that experienced widespread tree mortality during this drought.

40 We conduct a sensitivity analysis to explore how different plant water sourcing and hydraulic  
41 strategies lead to differential responses during normal and drought conditions.

42 The analysis shows that:

- 43 1) deep roots that sustain productivity through the dry season are needed for the model  
44 to capture observed seasonal cycles of ET and GPP in normal years, and that deep-  
45 rooted strategies are nonetheless subject to large reductions in ET and GPP when  
46 the deep soil reservoir is depleted during extreme droughts, in agreement with  
47 observations.
- 48 2) risky stomatal strategies lead to greater productivity during normal years as  
49 compared to safer stomatal control, but lead to high risk of xylem embolism during  
50 the 2012-2015 drought.
- 51 3) for a given stand density, the stomatal and xylem traits have a stronger impact on  
52 plant water status than on ecosystem level fluxes.

53 Our study reveals the importance of resolving plant water sourcing strategies in order to  
54 represent drought impacts on plants, and consequent feedbacks, in models.

55

56



## 57 **1. Introduction**

58 Understanding plant water use strategies and the resulting ecohydrologic processes in  
59 forests is critical for predicting surface water and energy exchange, carbon dynamics and  
60 vegetation dynamics of water-constrained ecosystems in a changing climate. Mediterranean-  
61 type climates, as in California, are characterized by dry and hot summers and cool, wet winters,  
62 resulting in asynchronous supplies of energy and water. In addition to these climatic stresses,  
63 plants in California are further subject to high inter-annual variability in precipitation, and  
64 periodic severe drought events, such as the recent 2012 – 2015 drought, which led to widespread  
65 tree mortality (Fettig et al. 2019). Together, these two climatic constraints bring a unique  
66 challenge to the success of forests in California, which are likely to be exacerbated in a warming  
67 climate.

68 On evolutionary timescales, natural selection has led to a wide array of strategies and  
69 functional traits that allow plants to both grow and survive under a range of environment  
70 conditions (Grime 1977,1979; Coley et al. 1985; Westoby et al. 2002; Craine 2002; Reich et al.  
71 2003). Given the centrality of water sourcing on plant physiology, plant hydraulic traits play an  
72 important role in water-constrained ecosystems. Once absorbed by fine roots, water flows  
73 through the vascular system via coarse roots, stems, branches, to leaves where it evaporates  
74 through stomata. The rate of water flow through stems, and thus the supply to leaves, is  
75 determined by the hydraulic conductivity along this pathway. If the water potential of xylem  
76 tissue becomes too low, cavitation can occur and cause a loss of conductivity. Because this  
77 cavitation can damage the xylem network, trees have developed different strategies to mitigate  
78 this effect, all of which come at some cost. These strategies include 1) early stomatal closure or  
79 leaf deciduousness to reduce the flow of water, at the cost of reduced carbon intake; 2) building  
80 cavitation-resistant xylem, at the cost of increased hydraulic resistance; and 3) growing deep  
81 roots to access more moisture, at the cost of higher carbon investment. In this study, we focus on  
82 the potential hydraulic strategies that trees in Californian ecosystems use, with a particular  
83 emphasis on how the co-ordination of hydraulic functional traits at the leaf, stem, and root levels  
84 is critical to carbon assimilation, transpiration, and consequently, the productivity and the  
85 response of trees to drought (Matheny, Mirfenderesgi, and Bohrer 2017; Matheny et al. 2017;  
86 Mursinna et al. 2018a).



87           The traits that regulate stomatal conductivity are the most important hydraulic traits of  
88 leaves and the primary ones through which photosynthesis and transpiration are coupled.  
89 Stomatal behavior falls along a gradient between two extremes: stomata may close early during  
90 water stress to avoid the risk of hydraulic failure, or remain open to maximize carbon uptake  
91 while exposing xylem to a higher risk of embolism (Martínez-Vilalta, Sala, and Piñol 2004;  
92 McDowell et al., 2008; Skelton, West, & Dawson, 2015, Matheny et al. 2017). The sensitivity of  
93 stomata to water stress determines where the stomata operate along the safety-risky gradient,  
94 thus the degree that carbon intake is traded for preventing the cavitation of xylem. Where the  
95 best stomatal strategy sits along the safety-risky gradient would depend on the physical  
96 environment.

97           The maximum hydraulic conductivity and the vulnerability to cavitation are the two key  
98 xylem hydraulic traits. Differences in the anatomy and morphology of the conductive xylem cell  
99 structure and anatomy (Hacke et al. 2017) lead to differences in maximum conductivity and the  
100 water potential at which cavitation starts to occur (Pockman & Sperry, 2000; Sperry 2003).  
101 Within the conifers, there are at least three mechanisms that lead to a tradeoff between xylem  
102 safety and efficiency. First is the morphology of the xylem conduit. It is widely acknowledged  
103 that narrow (or short) tracheid are safer than wider (or longer) tracheid but have lower  
104 conductance per sap area (Choat and Pittermann 2009). Second are the intervessel pit  
105 membranes. Thicker and less porous membranes prevent the spread of air but increase the  
106 hydraulic resistance of xylem (e.g. Li et al., 2016; Pratt & Jacobsen 2017). The third comes from  
107 the division of limited space (Pratt and Jacobsen 2017). With the same cross sectional area of  
108 conduits, vessels with a thicker cell wall provide stronger mechanical support, so that the  
109 conduits are less likely to collapse when xylem water potential becomes more negative, however  
110 this reduces the area that can be used for conduits transporting water. While these physiological  
111 constraints require that the tradeoff does exist to some extent, in many studies, this tradeoff  
112 appears to be weak, and there are certainly species that have both safe and efficient xylem.  
113 Further, there are many other plant traits can affect the safety such as wood density (Pratt and  
114 Jacobsen 2017), pit anatomy (Sperry & Hacke 2004, Lens et al. 2011), and biochemistry (Gortan  
115 et al. 2011). These traits can have large variation among the plant types. The tradeoff will be  
116 weakened when grouping plants in coarse scale, e.g by biomass, families and/or across a range of  
117 geological and climatic region. But when focusing on certain species in a particular region, the



118 tradeoff becomes stronger, as demonstrated by many local studies (e.g. Barnard et al. 2011,  
119 Corcuera et al. 2011, Baker et al. 2019). For example, Kilgore et al. (2021) shows that there is  
120 clear safety-efficiency tradeoff of the pine trees in a specific location in the western US. Thus,  
121 while we acknowledge that there are many exceptions to the xylem safety-efficiency tradeoff, it  
122 is a useful framework for examining plant strategies for dealing with drought.

123 The traits that govern the hydraulic function of plant root systems are also critically  
124 important but the least understood and studied. These traits include the rooting depth, the root to  
125 shoot ratio, the vertical and lateral distribution of roots, and the fine root density and diameters,  
126 all of which are related to water uptake (Canadell et al., 2007, Allen 2009, Reichstein et al.,  
127 2014, Wullschleger et al. 2014). In general, species with deeper roots can access water at greater  
128 depths that is unavailable to more shallowly rooted species (Jackson et al., 1996; Canadell et al.,  
129 1996). The vertical root distribution can affect the water uptake and thus the evapotranspiration  
130 pattern during the dry-down period (Teuling, Uijlenhoet, and Troch 2006). This in turn affects  
131 the seasonal distribution of water over the soil depth, and thereby the resilience of plants to  
132 seasonal droughts (Yu, Zhuang, and Nakayamma 2007). The vertical root distribution is also a  
133 means of belowground niche differentiation (Ivanov et al. 2012; Kulmatiski and Beard 2013),  
134 whereas the extent of the lateral root distribution dictates the competition of water (Agee et al.  
135 2021). Whether a plant can benefit from having deep roots is related to the plant's leaf and xylem  
136 hydraulic traits (e.g. Johnson et al. 2018, Mackay et al. 2020), thus requiring coordination of  
137 rooting and hydraulic traits.

138 Given the strength of the Mediterranean-type climate of California, the coordination of  
139 rooting and hydraulic strategies will play a critical role for the forest dynamics. However, the  
140 interplay of rooting and hydraulic strategies and their impact on ecosystem processes haven't  
141 been well understood. In this study, we address this question at the Soaproot site (CZ2) of the  
142 southern Sierra Nevada of California as the study area. The CZ2 site was strongly affected by the  
143 2012-2015 drought, with extremely high tree mortality rates (~90% of the pine died) (Fettig et al.  
144 2019). While the 2012 - 2015 drought was widespread across California, the highest rates of tree  
145 mortality occurred in the southern Sierra Nevada, centered around an elevation similar to this site  
146 (1160 m to 2015 m, Asner et al. 2016, Goulden and Bales 2019). This mid-elevation region is  
147 also characterized by the highest forest productivity along an elevation gradient from foothill



148 woodlands to subalpine forest (Kelly and Goulden 2016). This leads us to ask whether strategies  
149 associated with high productivity exposed trees to high mortality risk under prolonged drought.

150 Specifically, here we use the Functionally Assembled Terrestrial Ecosystem Simulator, in  
151 a configuration that includes plant hydraulics (FATES-Hydro), to explore the tradeoffs  
152 associated with differing hydraulic strategies, and in particular their implications for plant  
153 productivity and risk of drought-induced mortality. We conduct a sensitivity analysis, using  
154 FATES-Hydro in comparison with observations from the CZ2 eddy covariance site, to  
155 investigate how stomatal, xylem and rooting strategies affect the ecosystem and physiologic  
156 processes of the forest, and whether that may explain the high rates of both productivity and  
157 drought-associated mortality of conifers at CZ2.

## 158 **2. Methods**

### 159 2.1 Study site

160 The Soaproot site is a 543-ha headwater catchment at 1100m elevation (37°2.4' N,  
161 119°15.42' W), which is at the lower boundary of the rain–snow transition line with warm, dry  
162 summers and cool, wet winters (Geen et al. 2018). The mean annual temperature is about 13.8°C  
163 (Goulden et al., 2012). Under normal conditions, the annual precipitation is about 1300 mm, but  
164 during a dry year, the precipitation can drop to 300-600mm. (Bales et al. 2018). The site is a  
165 ponderosa pine (*Pinus ponderosa*) dominated conifer ecosystem exhibiting high productivity  
166 (Kelly and Goulden (2016) reported 2.1 tC/ha/year average annual gross stem wood production  
167 averaged). Other species include California black oak (*Quercus kelloggii* Newberry), and incense  
168 cedar (*Calocedrus decurrens*).

169 Soils at the Soaproot site are mainly of the Holland (fine-loamy, mesic Ultic Haploxeralfs)  
170 and Chaix (coarse-loamy, mesic Typic Dystroxerepts) series, which are representative of soils  
171 across a similar elevation band of the western Sierra Nevada (Mooney and Zavaleta 2003). Soils  
172 of the Holland series have sandy loam surface texture and underlying Bt horizons with sandy  
173 clay loam textures, while soils of the Chaix series have sandy loam textures throughout the  
174 profile. The regolith depth is estimated to be 15m (Holbrook et al., 2014). The total porosity over  
175 the whole regolith depth of the site is estimated to be 1620 mm and the total available storage  
176 porosity (plant accessible water storage capacity), which is the difference in volumetric water



177 content between field capacity and permanent wilting point (~ -6Mpa) to be 1400 mm (Klos et  
178 al. 2017). The available water storage capacity is approximately  $0.20 \text{ cm}^3 \text{ cm}^{-3}$  in the upper  
179 regolith (0–5 m depth) which decreases to  $0.05 \text{ cm}^3 \text{ cm}^{-3}$  or less in the lower regolith (below 5 m  
180 depth) (Holbrook et al., 2014).

181 An eddy-covariance flux tower was installed at this site in September 2010. The elevation  
182 of the tower is 1160 m above sea level. Instruments on the flux tower track changes in carbon  
183 dioxide, water vapor, air temperature, relative humidity, and other atmospheric properties. We  
184 compare the simulated gross primary productivity and latent heat flux with the flux tower  
185 measurements over the period from 2011 to 2015 (Goulden and Bales 2019). We computed the  
186 Root Mean Square Error (RMSE) of the hourly mean diurnal cycle of each month. This allows  
187 us to examine the capacity of FATES-Hydro to predict the carbon and water fluxes. The  
188 transpiration of the site contributed to the majority of the ET as indicated by the measurements  
189 from an adjacent catchment, as well as the fact that the site is fully vegetated with an annual LAI  
190 around 3 to 4.

191

## 192 2.2 FATES-Hydro model and parameterization

### 193 2.2.1 The FATES-Hydro model

194 FATES is a cohort-based, size- and age-structured dynamic vegetation model, where long-  
195 term plant growth and mortality rates and plant competition emerge as a consequence of  
196 physiological processes. FATES is coupled within both the CLM5 (Lawrence et al., 2019) and  
197 the ELM (Golaz et al., 2020) land surface models (LSMs). In this study, FATES is coupled with  
198 the CLM5. FATES-Hydro is a recent development of the FATES model (Fisher et al., 2015;  
199 Koven et al., 2020), in which a plant hydro-dynamic module, originally developed by  
200 Christoffersen et al. (2016), was coupled to the existing photosynthesis and soil hydraulic  
201 modules.

202 Conceptually, plant hydraulic modules can be broadly grouped into to two types. The first  
203 group represents plant hydraulic system as analogous to an electrical circuit (e.g. Mackay et al.  
204 2011, Eller et al. 2018, Kennedy et al. 2019). The total resistance of the plant is calculated from  
205 the resistance of each compartment using Ohm's law. There is no storage of water in the plants



206 and the transpiration from plants at any given time step is considered to be completed from soil  
207 storage. The second group represents plant hydraulics by a series of connected porous media,  
208 corresponding to each plant compartment (e.g. Bohrer et al. 2005), Janott et al. 2011, Xu et al.,  
209 2016, Christoffersen et al., 2016). The porous media model takes into account the water storage  
210 in the plant. The flow between two adjacent compartments is driven by the difference in the  
211 water potential, mediated by the hydraulic conductivity. FATES-Hydro falls in the second group.  
212 The models in the second group differ in the exact formulas used to describe the pressure-  
213 volume and pressure-conductivity relations, as well as different numbers and arrangement of  
214 nodes within the soil-plant-atmosphere system.

215 In FATES-Hydro, for each plant cohort, the hydraulic module tracks water flow along a  
216 soil–plant–atmosphere continuum of a representative individual tree based on hydraulic laws,  
217 and updates the water content and potential of leaves, stem, and roots with a 30 minute model  
218 time step. Water flow from each soil layer within the root zone into the plant root system is  
219 calculated as a function of the hydraulic conductivity as determined by root biomass and root  
220 traits such as specific root length, and the difference in water potential between the absorbing  
221 roots and the rhizosphere. The vertical root distribution is based on Zeng's (2001) two parameter  
222 power law function which takes into account the regolith depth:

$$223 \quad Y_i = \frac{0.5(e^{-r_a z_{li}} + e^{-r_b z_{li}}) - 0.5(e^{-r_a z_{ui}} + e^{-r_b z_{ui}})}{1 - 0.5(e^{-r_a z} + e^{-r_b z})} \quad (\text{Eq 1})$$

224 where  $Y_i$  is the fraction of fine or coarse roots in the  $i$ th soil layer,  $r_a$  and  $r_b$  are the two  
225 parameters that determine the vertical root distribution,  $Z_{li}$  is the depth of the lower boundary of  
226 the  $i$ th soil layer, and  $Z_{ui}$  is the depth of the upper boundary of the  $i$ th soil layer, and  $Z$  is the total  
227 regolith depth. The vertical root distribution affects water uptake by the hydrodynamic model by  
228 distributing the total amount of root, and thus root resistance, through the soils.

229 The total transpiration of a tree is the product of total leaf area (LA) and the transpiration  
230 rate per unit leaf area (J). In this version of FATES-Hydro, we adopt the model developed by  
231 Vesala et al. (2017) to take into account the effect of leaf water potential on the within-leaf  
232 relative humidity and transpiration rate:





$$E = LA \cdot J \quad (\text{Eq 2a})$$

$$J = \rho_{\text{atm}} \frac{(q_l - q_s)}{1/g_s + r_b} \quad (\text{Eq 2b})$$

$$q_l = \exp\left(\frac{k_{LWP} \cdot LWP \cdot V_{H_2O}}{R \cdot T}\right) \cdot q_{\text{sat}} \quad (\text{Eq 2c})$$

234 where  $E$  is the total transpiration of a tree,  $LA$  is the total leaf area ( $\text{m}^2$ ),  $J$  is the transpiration per  
235 unit leaf area ( $\text{kg s}^{-1} \text{m}^{-2}$ ),  $\rho_{\text{atm}}$  is the density of atmospheric air ( $\text{kg m}^{-3}$ ),  $q_l$  is the within-leaf  
236 specific humidity ( $\text{kg/kg}$ ),  $q_s$  is the atmosphere specific humidity ( $\text{kg/kg}$ ),  $g_s$  is the stomatal  
237 conductance per leaf area,  $r_b$  is the leaf boundary layer resistance ( $\text{s m}^{-1}$ ),  $k_{LWP}$  is a scaling  
238 coefficient (unitless), which can vary between 1 and 7, and here we use a value of 3;  $LWP$  is the  
239 leaf water potential (Mpa),  $V_{H_2O}$  is the molar volume of water ( $18 \times 10^{-6} \text{m}^3 \text{mol}^{-1}$ ),  $R$  is the  
240 universal gas constant, and  $T$  is the leaf temperature (K).

241 The sap flow from absorbing roots to the canopy through each compartment of the tree  
242 along the flow path way (absorbing roots, transport roots, stem, and leaf) is computed according  
243 to Darcy's law in terms of the plant sapwood water conductance, the water potential gradient:

$$Q_i = -K_i [\rho_w g (z_i - z_{i+1}) + (\Psi_i - \Psi_{i+1})] \quad (\text{Eq 3})$$

245 where  $\rho_w$  is the density of water;  $z_i$  is the height of the compartment (m);  $z_{i+1}$  is the height  
246 of the next compartment down the flow path (m);  $\Psi_i$  is the water potential of the  
247 compartment (Mpa);  $\Psi_{i+1}$  is the water potential of the next compartment down the flow  
248 path (Mpa); and  $K_i$  is the hydraulic conductivity of the compartment ( $\text{kg/Mpa/m/s}$ ). The  
249 hydraulic conductivity of the compartments is by the water potential and maximum hydraulic  
250 conductivity of the compartment through the pressure-volume (P-V) curve and the vulnerability  
251 curve (Manzoni et al. 2013, Christoffersen et al. 2016).

252 The plant hydrodynamic representation and numerical solver scheme within FATES-  
253 HYDRO follows Christoffersen et al. (2016). We made a few modifications to accommodate the  
254 multiple soil layers and to improve the numerical stability. First, to accommodate the multiple  
255 soil layers, we have sequentially solved the Richards' equation for each individual soil layer,  
256 with each layer-specific solution proportional to each layer's contribution to the total root-soil



257 conductance. Second, to improve the numerical stability, we have an option to linearly  
258 extrapolate the PV curve beyond the residual and saturated tissue water content to avoid the rare  
259 cases of overshooting in the numerical scheme under very dry or wet conditions. Third,  
260 Christoffersen et al. (2016) use three phases to describe the PV curves: 1) dehydration phases  
261 representing capillary water (sapwood only), 2) elastic cell drainage (positive turgor), and 3)  
262 continued drainage after cells have lost turgor. Due to the possible discontinuity of the curve  
263 between these three phases, it leads to the potential for numerical instability. To resolve this  
264 instability, FATES-HYDRO added the Van Genuchten model (Van Genuchten 1980, July and  
265 Horton 2004) and the Campbell model (Campbell 1974) as alternatives to describe the PV  
266 curves.

267 In this study, we use the Van Genuchten model because of two advantages: 1) it is simple,  
268 with only three parameters needed for both curves, and 2) it is mechanistically based, with both  
269 the P-V curve and vulnerability curve derived from a pipe model, and thus connected through  
270 three shared parameters:

$$\Psi = \frac{1}{-\alpha} \cdot \left( \frac{1}{Se^{1/m}} - 1 \right)^{1/n} \quad (\text{Eq 4a})$$

271

$$FMC = \left( 1 - \left( \frac{(-\alpha \cdot \Psi)^n}{1 + (-\alpha \cdot \Psi)^n} \right)^m \right)^2 \quad (\text{Eq 4b})$$

272 where  $\Psi$  is the water potential of the media (xylem in this case) (Mpa);  $FMC$  is the fraction of  
273 xylem conductivity,  $K/K_{\max}$ , (unitless);  $\alpha$  is a scaling parameter for air entry point ( $\text{Mpa}^{-1}$ ),  $Se$   
274 is the dimensionless standardized relative water content as  $Se = (\theta - \theta_r) / (\theta_{sat} - \theta_r)$  with  $\theta$ ,  $\theta_r$ ,  $\theta_{sat}$   
275 are volumetric water content ( $\text{m}^3 \text{m}^{-3}$ ), residual volumetric water content, and saturated  
276 volumetric water content correspondingly; and  $m$  and  $n$  are dimensionless (xylem conduits) size  
277 distribution parameters. The model assumes that xylem conductance can be restored as xylem  
278 water content increases due to increased water availability after a dry period without any  
279 hysteresis in the FMC curve.

280



281 The stomatal conductance is modelled in the form of the Ball-Berry conductance model  
282 (Ball et al. 1987, Oleson et al. 2013, Fisher et al. 2015):

$$283 \quad g_s = b_{slp} \frac{A_n}{c_s / P_{atm}} \frac{e_s}{e_i} + b_{opt} \beta_t, \quad (\text{Eq 5})$$

284 where  $b_{slp}$  and  $b_{opt}$  are parameters that represent the slope and intercept in the Ball-Berry model,  
285 correspondingly. These terms are plant strategy dependent and can vary widely with plant  
286 functional types (Medlyn et al. 2011). The parameter  $b_{opt}$  is also scaled by the water stress index  
287  $\beta_t$ .  $A_n$  is the net carbon assimilation rate ( $\mu\text{mol CO}_2 \text{ m}^{-2} \text{ s}^{-1}$ ) based on Farquhar's (1980)  
288 formula. This term is also constrained by water stress index  $\beta_t$  in the way that the  $V_{\text{cmax},25}$  is  
289 scaled by  $\beta_t$  as  $V_{\text{cmax},25}\beta_t$  (Fisher et al. 2018).  $c_s$  is the  $\text{CO}_2$  partial pressure at the leaf surface  
290 (Pa),  $e_s$  is the vapor pressure at the leaf surface (Pa),  $e_i$  is the saturation vapor pressure (Pa) inside  
291 the leaf at a given vegetation temperature when  $A_n = 0$ .

292 The water stress index  $\beta_t$ , a proxy for stomatal closure in response to desiccation, is  
293 determined by the leaf water potential adopted from the  $\text{FMC}_{gs}$  term from Christoffersen et al.  
294 (2016):

$$295 \quad \beta_t = \left[ 1 + \left( \frac{\Psi_l}{P50_{gs}} \right)^{a_{gs}} \right]^{-1} \quad (\text{Eq 6})$$

296 where  $\Psi_l$  is the leaf water potential (MPa),  $P50_{gs}$  is the leaf water potential of 50% stomatal  
297 closure, and  $a_{gs}$  governs the steepness of the function. For a given value of  $a_{gs}$ , the  $P50_{gs}$  controls  
298 the degree of the risk of xylem embolism (Christoffersen et al. 2016, Powell et al. 2017). A more  
299 negative  $P50_{gs}$  means that, during leaf dry down from full turgor, the stomatal aperture stays  
300 open and thus allows the transpiration rate to remain high and xylem to dry out, which thus can  
301 maintain high photosynthetic rates, at the risk of exposing xylem to embolism and thus plant  
302 mortality. Conversely, a plant with a less negative  $P50_{gs}$  will close its stomata quickly during  
303 leaf dry down, thus limiting transpiration and the risk of xylem embolism and mortality  
304 associated with it, at the cost of reduced photosynthesis.

305



## 306 2.2.2 Sensitivity analysis and Parameterization

307 The goal of this analysis is to better understand how coordinated aboveground and  
308 belowground hydraulic traits determine plant physiological dynamics and the interplay between  
309 ecosystem fluxes and tissue moisture during the extreme 2012-2015 drought at the Soaproot site.  
310 We thus conduct a global sensitivity analysis on selected hydraulic parameters to explore the  
311 linkages of aboveground and belowground hydraulic strategies. We use a full-factorial design for  
312 the parameter sensitivity analysis in order to best investigate the relationships between  
313 parameters. Because this design requires a relatively small set of parameters or groups of  
314 parameters to vary, we chose parameters that represent the major axes of relatively well  
315 understood stomatal, xylem and rooting mechanisms/strategies that control the hydraulic  
316 functioning of trees. We set the values of these parameters within the realistic range based on  
317 online database, and literatures where the species and physical environment are as close to our  
318 system as possible. We list other major parameters and their estimates that are not varied in the  
319 sensitivity analysis (table 2).

320 The parameters that we vary here are 1) the pair of  $r_a$  and  $r_b$ , which control vertical root  
321 distribution as deep vs shallow roots, 2) two sets of xylem parameters ( $P_{50x}$ ,  $K_{max}$ ,  $m$ ,  $n$ , and  $\alpha$ )  
322 that represent two distinct xylem strategies: efficient/unsafe and inefficient/safe xylem within the  
323 range observed for temperate conifer trees, and 3) the stomatal parameter  $P50_{gs}$ , which represents  
324 the stomatal strategy along a risky to safe gradient (Table 1). The ranges of root parameters are  
325 chosen so that the effective rooting depth, above which 95% of root biomass stays, varies from  
326 1m to 8m which is the possible range at the Soaproot site, as indicated by current knowledge of  
327 the subsurface structure (see Klos et al., 2017). Note, here we refer to a higher proportion of  
328 roots in deep subsurface layers as ‘deep rooting’ (e.g effective rooting depth = 8m;  $r_a=0.1, r_b=0.1$ )  
329 as compared to ‘shallow rooting’ (e.g effective rooting depth = 2;  $r_a=1, r_b=5$ ) which represents a  
330 larger proportion of fine roots in upper layers (Figure 1a).

331 The safety-efficiency tradeoff of xylem has been widely discussed in the literature (e.g.  
332 Gleason et al. 2016; Hacke et al. 2006, 2017; Martnez-Vilalta, Sala, and Piol 2004). Given that  
333 we don’t have any measurements that can be used to generate vulnerability curve at our study  
334 site, we consult the literature (Domec et al. 2004, Barnard et al. 2011, Corcuera et al. 2011,  
335 Anderegg and Hillerislambers 2016, Baker et al. 2019, Kilgore et al. 2021) for observed curves



336 from sites that have as similar climate (e.g mean annual precipitation and temperature) and  
337 conifer species (*P. Ponderosa*) to our study site as possible and the values of xylem traits ( $K_{max}$   
338 and  $P50_x$ ) of *Ponderosa* pine in temperate regions of the TRY database (Kattge et al. 2020) to  
339 determine the two hypothetical vulnerability curves representing the safe/inefficient and  
340 unsafe/efficient xylem strategies. We set the parameters of the van Genuchten model to represent  
341 these two sets of P-V and vulnerability curves as showing in Fig1b and 1c. It is worth noting that  
342 with the same  $K_{max}$  and  $P50$ , the exact shape of the vulnerability can be different depends on the  
343 formula used and parameter values. However, this should not be an issue in our study because  
344 vulnerability curve is mainly constrained by  $P50$  and  $K_{max}$ . Second, given there is a large range  
345 of variation of the observed/measured values, the effect caused by the exact shape of the curves  
346 is minor. Third, since the objective of our study is not to accurately predict mortality, but rather  
347 to examine the effect of different combination of stoma, xylem, and root strategies, even if the  
348 shape of our vulnerability curve is not the most accurate, as long as the curve captures the overall  
349 pattern of the pressure-conductivity relation, it will not affect the relative outcome of this study.

350 We follow the theory of Skelton et al. (2015) to define safe vs. efficient stomatal strategy.  
351 In FATES-Hydro, there are two key stomatal parameters:  $P50_{gs}$  and  $a_{gs}$ . Here, we only vary  
352  $P50_{gs}$  while keeping  $a_{gs}$  as a constant because the objective here is to choose the parameters that  
353 are relatively well understood and catch the safe vs. risky strategies as described by Skelton et  
354 al., rather than to exhaust the parameter space throughout the model. In essence, the different  
355 combinations of  $P50_{gs}$  and the shape parameter ( $a_{gs}$ ) can generate similar stomatal response  
356 curves. For example, a small negative  $P50_{gs}$  with small  $a_{gs}$  would result in a flat stomatal  
357 response curve, which is similar to a large negative  $P50_{gs}$  combined with a large  $a_{gs}$ . Further,  
358  $P50_{gs}$  is well understood and has more observed data, while  $a_{gs}$  is less studied and barely has any  
359 observed data. With a given  $a_{gs}$ , the variance of  $P50_{gs}$  along a vulnerability curve controls the  
360 degree of embolism risk, from a ‘risky’ strategy, where  $P50_{gs}$  equals to a lower  $P_{xylem}$ , to a  
361 ‘conservative’ strategy, where  $P50_{gs}$  equals a higher  $P_{xylem}$ . The  $P_{xylem}$ s in Skelton et al.’s (2015)  
362 are for Fynbos species, therefore are not appropriate for our study because our species are pine  
363 trees, a woody plant. Trees have woody tissue which contribute to strengthen the conduits and  
364 make them less easy to collapse when embolized, hence allow their stomata to be riskier than  
365 herbaceous plants. From the observed  $P50_{gs}$  and xylem traits of closely related pine species in  
366 the TRY database (Kattge et al. 2020) and elsewhere in the literature (Bartlett et al. 2016), as



367 well as the observed soil water potential at the study site, we choose to vary  $P50_{gs}$  between  
368  $P50_{xylem}$  and  $P20_{xylem}$ , (correspondingly the point at which xylem have lost 50% and 20% of their  
369 maximum conductivity).

370 The emergent behavior of FATES or any model with dynamic ecosystem structure can  
371 make analysis of physiological rate variation difficult, as the stand structure will respond and  
372 thus also vary when parameters are changed. To overcome this complication, we use a reduced  
373 complexity configuration for running the model which we refer to as ‘static stand structure’  
374 mode. In this mode, the stand structure is initialized from observed forest census data, and  
375 subsequently is fixed, i.e. the model does not permit plant growth or death to change the  
376 vegetation structure. This allows the direct assessment of hydraulic and physiological parameter  
377 variation in the model without the consequent feedback loops associated with varying ecosystem  
378 structure. The stand structure is initialized with census data from the CZ2 site (Table S1).  
379 Because this type of model configuration ignores prognostic plant mortality, in the interest of  
380 being able to compare across simulations where mortality rates might otherwise be very high, we  
381 use the loss of xylem conductivity as a measure of mortality risk of conifer trees at CZ2, which  
382 has widely been used as an indicator of drought mortality of forest (e.g. Hammond et al., 2019).

383 To force the model with an atmospheric upper boundary, we use the Multivariate Adaptive  
384 Constructed Analogs (MACA) climate data (Abatzoglou and Brown 2012) from 2008 – 2015 of  
385 a 4km x 4km grid covers the study area. The daily average MACA data are disaggregated to 3-  
386 hourly climate data (see Appendix S2 in Buotte et al. 2018 for detail) . To assess the credibility  
387 of model predictions, we compare the model to observations of gross primary productivity (GPP)  
388 and ET, both as inferred from eddy covariance (Goulden and Bales 2019). Here, we use the  
389 Latent Heat Flux (LH) is used as a proxy of ET.

### 390 **3. Results**

#### 391 3.1 Impact on GPP and ET

392 The parameter sensitivity analysis shows that in a monthly-mean flux comparison, the  
393 simulations with deep roots give a better match to the overall observed pattern of GPP and ET  
394 (Fig. 2). The simulated transpiration contributes to 90% of the ET in general. The deep-rooted  
395 cases better capture the seasonality (e.g. the peak time) and the declining trend of observed GPP



396 from 2011 to 2015. The deep-rooted cases also match fairly well the observed ET. The simulated  
397 GPP of shallow-rooted cases are higher than observed values during wet seasons (Dec. to Mar.),  
398 but much lower than the observed values during dry season of the pre-drought period. The  
399 simulated ET of shallow-rooted cases are overall lower than the observed values. To quantify  
400 this assessment, we computed Root Mean Square Error (RMSE) from the hourly mean GPP and  
401 ET of each month each year of all the 40 cases (Fig. S2). The RMSE of GPP and ET decreases  
402 with effective rooting depth and P50gs for both xylem strategies (Fig. 3). The P50gs has less  
403 impact on RMSE of GPP of the safe xylem than on that of the efficient xylem. In terms of GPP,  
404 the effective rooting depth of 6.5m gives the best fit, as indicated by the darkest color (RMSE of  
405 GPP =  $1.12\text{gC/m}^2/\text{s}$ , RMSE of ET =  $250\text{ W/m}^2$ ), suggesting the importance of deep roots in  
406 maintaining transpiration and photosynthesis during the dry season, as well as increasing the  
407 relative decline in these fluxes during the drought.

408 Among the parameters we varied in the sensitivity analysis, the vertical root distribution  
409 has the largest impact on GPP and ET at CZ2. Figures 2a-2b show the monthly mean GPP and  
410 ET of the end members of the sensitivity analysis (see Fig. S1 for the complete set of outcomes).  
411 Deep roots result in substantially higher GPP and transpiration during normal years (2011 and  
412 2012). During long-term droughts, when deep soil moisture is depleted, the relative advantage of  
413 deep roots over shallow roots is reduced. Shallow roots result in substantially lower GPP and  
414 transpiration during the dry season (Aug. to Oct.), with seasonal maximum occurring earlier, in  
415 May, as compared to July with the deep-rooted cases. The shallow-rooted cases also have much  
416 lower GPP and ET during the dry seasons of the pre-drought period. During the late stage of  
417 drought (2014 and 2015), the GPP and ET of the different cases become more similar between  
418 the shallow- and deep-rooted cases.

419 The second set of parameters in importance to rooting depth for controlling carbon and  
420 water fluxes is the stomatal strategy. The simulations with a more risky strategy ( $P50_{gs}=P50_x$ )  
421 gives higher GPP and ET than the simulations with a safer strategy ( $P50_{gs}=P20_x$ ) during pre-  
422 drought periods and the early stage of the drought (2011 to 2013), but slightly lower GPP and ET  
423 at the late stage of the drought (2014 and 2015) for the deep-rooted cases. However, risky  
424 stomata gives slightly higher GPP and ET at all times for shallow-rooted cases. The xylem  
425 strategy has the smallest effect on GPP and ET of the parameters we varied (e.g RMSEs of ET



426 are both around 260 W/m<sup>2</sup> for safe and efficient xylem respectively, with P50<sub>gs</sub> = P20<sub>x</sub> and 8m  
427 effective rooting depth). In deep-rooted cases, the safe xylem and efficient xylem strategy result  
428 in almost the same GPP and ET, which can be seen via the widespread overlap between the  
429 dashed and solid lines in figure 1. In shallow-rooted cases, with safe stomata, safe xylem  
430 generates slightly higher GPP and ET than efficient xylem. In addition, how strong the effects of  
431 stomatal and xylem strategy also depend on the rooting depth. The deeper the effective rooting  
432 depth, the less significant the impacts of stomatal strategy (Fig. S1).

433

### 434 3.2 Impact on plant water status

435 We examine the impact of vertical root distributions, stomatal and xylem strategies on the  
436 seasonal variation of three plant physiologic variables that serve as indices of plant water stress  
437 (fig. 4): the fraction loss of xylem conductivity of stem (SFL), leaf water potential (LWP), and  
438 an overall absorbing roots water potential (AWP). In the model, absorbing roots in different soil  
439 layers have different water potentials, associated with the soil water potential of that layer. We  
440 calculate a cohort-level effective AWP as the root-fraction weighted average of water potential  
441 in absorbing root across all soil layers. In this way, the AWP represents the overall rhizosphere  
442 soil moisture condition that is sensed by the tree. These physiological variables are tracked for  
443 each cohort. For any given case, the differences in these variables among cohorts are negligible  
444 (Fig. S3). Therefore, we present the outcome of the cohort class with a diameter at breast height  
445 (DBH) between 50 – 60cm, the size class that is most abundant at CZ2.

446 Stomatal and rooting strategies together control the loss of xylem conductivity during the  
447 dry season of the pre-drought period and the whole period of the long-term drought (Fig 4a). In  
448 all cases, the xylem conductivity reaches a maximum during the wet season (Dec. to Jan.), starts  
449 to decline during the growing season (Apr. to Jun.), then reaches its minimum in the dry season.  
450 With the same stomatal strategy, deep roots lead to less loss of xylem conductivity than shallow  
451 roots. A deep rooting strategy is also able to maintain very little loss of xylem conductivity  
452 during the pre-drought period, but as deep soil moisture is depleted, this effect is reduced. With a  
453 shallow rooting profile, the xylem conductivity starts to decline earlier and the minimum is much  
454 lower than that of a deep rooting profile. For example, with risky stomata, the minimum fraction  
455 of xylem conductivity of deep-rooted cases at 2012 is 0.4, but is lower than 0.2 with shallow





456 roots. Unlike deep-rooted cases, in shallow-rooted cases, the seasonal variation of the loss of  
457 xylem conductivity does not differ too much during pre-drought and drought periods. During  
458 very late stage of drought, deep-rooted cases have a lower fraction of xylem conductivity than  
459 shallow-rooted cases (e.g. Jan. 2015).

460 In general, risky stomata cause a greater loss of xylem conductivity ( $K/K_{max}$ ) than safe  
461 stomata, but the extent depends on the vertical root distribution. The effect of the stomatal  
462 strategy is more obvious in shallow-rooted cases. Risky stomata combined with shallow roots  
463 results in increasing the duration of 50% loss of xylem conductivity, as well as the maximum  
464 loss of xylem conductivity during the dry season. With a deep rooting strategy, the difference in  
465 the percentage loss of xylem conductivity between safe stomatal and risky stomatal cases  
466 increases with the progression of the drought, but with a shallow rooting strategy this difference  
467 remains more or less the same over time. In addition, in 2011, a very wet year, with deep roots, a  
468 safe xylem strategy is able to maintain the maximum xylem conductivity even during dry season  
469 (Fig 4a). The impact of xylem strategy on the percentage loss of xylem conductivity is relatively  
470 weak. For both deep- and shallow-rooted cases, trees with safe xylem lose less xylem  
471 conductivity during the wet season but lose more conductivity during the dry season.

472 The safe stomata & safe xylem cases for both deep- and shallow-rooted trees experience  
473 greater declines in stem conductivity as compared to the safe stomata and efficient xylem for the  
474 corresponding rooting depths (Fig. 4a). This is because with safe stomata, trees operate at the  
475 right end of the vulnerability curve shown in fig. 1b, where the hydraulic conductivity of  
476 efficient xylem is much higher than that of the safe xylem. Thus, when transpiring the same  
477 amount of water, the efficient xylem will lose less water potential as compared to safe xylem.  
478 This keeps the xylem water potential of a plant with efficient xylem higher than one with safe  
479 xylem, and consequently also keeps the xylem conductivity,  $K$ , higher. This is also because we  
480 set  $P50_{gs}$  based on  $P_{xylem}$ , thus the  $P50_{gs}$  of safe stomata for plants with efficient xylem is higher  
481 (less negative) than that of plants with safe xylem, thus resulting in lower transpiration rates,  
482 which in term reduces the loss of xylem water potential. As a result, plants with both safe  
483 stomata and efficient xylem not only transpire less water but also lose less water potential per  
484 volume of water transpired. Together, these two mechanisms contribute to keep the xylem  
485 conductivity of the efficient xylem cases higher.



486 Stomatal, rooting, and xylem strategies have similar impacts on the seasonal variation of  
487 both leaf and fine root water potentials (Fig4c and 4d). Leaf and fine root water potentials peak  
488 during the winter, then start to decline in early spring and reach their lowest point in the dry  
489 season. Deep roots, safe stomata, and safe xylem traits all contribute to the maintenance of  
490 higher leaf and fine root water potentials during the growing and dry seasons. With deep roots,  
491 there is less difference in leaf and fine root water potential between stomatal and xylem  
492 strategies in the very wet year 2011. Plants that combine safe stomata and/or safe xylem with  
493 deep roots can keep the leaf and fine root water potentials relatively high (less than -5 Mpa)  
494 during the dry season of the drought period. However, while plants that combine risky stomata or  
495 efficient xylem with deep roots can keep the dry season leaf water potential above -5 Mpa during  
496 the pre-drought period, their traits lead to the dry season leaf water potential dropping below -8  
497 Mpa or even below -10 Mpa during the drought period. In both deep-rooted and shallow-rooted  
498 cases, safe xylem leads to much lower leaf and fine root water potentials during the dry season.  
499 The seasonal and inter-annual variation of fine root water potentials are almost identical to the  
500 leaf water potential, except that the water potential of fine roots is slightly higher (~ 0.5 Mpa)  
501 than the leaf water potential.

502

### 503 3.3 Impact on subsurface hydrology

504 In the simulation outcomes, the vertical root distributions again have the largest impact on  
505 hydrologic processes and subsurface water content and the way that they change over the  
506 drought. With deep roots, there is less drainage loss from surface and subsurface runoff as  
507 compared to shallow roots, especially during the growing season (Figure 5a,c,e,g). The  
508 subsurface water content shows different vertical and temporal patterns between the cases with  
509 different vertical root distributions. In the deep-rooted cases, during the pre-drought period, the  
510 water content in the deepest layers fluctuates between wet and dry seasonally; during the first  
511 year of the drought, the water content of the deepest layers (6 to 8m) slightly increases during the  
512 wet season, but with the progression of the drought, the soil water content becomes consistently  
513 depleted in the middle and deep layers (between 5 and 8 m depth) and only the shallow layer  
514 (<0.16 m) water content increases during wet season. In the shallow-rooted cases (Figure  
515 5b,d,f,h), soil moisture in the surface layers (top 2m) shows seasonal variation, but this seasonal



516 variation becomes weaker over depth and the soil moisture at 6-8m depth stays consistently high  
517 throughout the year during pre-drought period, and remains slightly low through the entire  
518 drought period; while the water content of the middle and upper layers of the shallow-rooted  
519 case have a similar pattern of seasonal variation before and during the drought.

520 Stomatal strategy, as quantified by  $P50_{gs}$ , has a weak impact on hydrologic processes and  
521 soil moisture. In both the deep- and shallow-rooted cases, riskier stomata lead to a slightly lower  
522 total subsurface water content (Figure 6a). The effect of  $P50_{gs}$  is less significant during the pre-  
523 drought period for both the deep-rooted and shallow-rooted cases, and becomes more significant  
524 as the drought progresses. The effect of  $P50_{gs}$  on total subsurface water content is less significant  
525 in shallow-rooted cases. Figure 5c shows the effect of  $P50_{gs}$  on the water content of shallow and  
526 deep soil layers. In both the shallow- and deep-rooted cases, increasing  $P50_{gs}$  has a negligible  
527 impact on the water content of the shallow layers during both the pre-drought and drought  
528 periods (Figure 5c left). For deeper layers, in the shallow-rooted case,  $P50_{gs}$  has no impact on the  
529 water content at all times; in the deep-rooted cases, a risky  $P50_{gs}$  results in lower dry season  
530 water content of deep layers (7-8m) during the pre-drought period (indicated by the red cycles of  
531 Figure 5a and 5c), but decreases the water content of those layers year round during the drought  
532 period (Figure 5a and 5e). In deep-rooted cases, safe stomata with efficient xylem lead to a  
533 slightly higher water content in deep layers (5m to 8m) during the pre-drought period, and in  
534 shallow layers (0 to 3m) during the drought period (Figure 6a). Risky stomata with safe xylem in  
535 deep-rooted cases are most effective in accessing soil water. Though the soil water contents are  
536 generally high in shallow-rooted cases, stomatal and xylem strategies show a similar impact on  
537 the soil water storage as those in the deep-rooted cases (Fig S4).

538 Simulations with deep roots have almost no loss of soil water to drainage during the dry  
539 season in normal years, or during the whole drought period; while with shallow roots, the  
540 drainage loss is high during the pre-drought period and decreases through the drought period, but  
541 still with some runoff even at the end of the drought period (Figure 6a). The observed total  
542 annual runoff from the 2008 to 2011 pre-drought period was about 250 mm/year, but was zero  
543 during the 2012 – 2015 drought period (from figure 4, Bales et al. 2018). This observed  
544 difference in runoff between the pre-drought (~290mm/year, 2011 - 2012) and drought periods  
545 (~0 mm/year) from the deep-rooted case is consistent with the predicted pattern. During the pre-



546 drought period, the wet season total subsurface water contents from Dec. to Feb. are similar  
547 between the cases with deep and shallow roots, but during the dry season (from June to Sep.) the  
548 total subsurface water content with shallow roots is substantially higher than the case with deep  
549 roots (Figure 6b).

#### 550 **4. Discussion**

##### 551 4.1 Vertical root distribution as the first order control

552 The outcome of our simulations indicates that the vertical root distribution exerts the first  
553 order control over both ecosystem level fluxes and plant physiology at CZ2. This dominance of  
554 rooting strategy over other hydraulic traits is related to the nature of the rainfall pattern of the  
555 Mediterranean-type climate of that region. The CZ2 site receives effectively all of its rain during  
556 winter. This water is stored in the soil column and slowly released through the growing season.  
557 The root zone soil moisture has strong seasonal variation, which constrains plant water use and  
558 gas exchange as a function of the gradual drying of the soil column (Bales et al., 2018). In the  
559 model, the stomatal behavior is controlled by the leaf water potential, which itself is strongly  
560 affected by the root zone soil moisture. In our simulations, the daytime average leaf water  
561 potential of a 55cm DBH cohort is well correlated with the fine root water potential and is  
562 always about 0.5 Mpa lower (fig S5). This offset is consistent with the relationship between mid-  
563 day leaf water potential and pre-dawn leaf water potential found by Martínez-Vilalta et al. (2014)  
564 at the global scale.

565 With deep roots, trees use more subsurface storage capacity at the CZ2 site, and thus a  
566 higher amount of total rainfall. In a wet year such as 2011, the root zone water potential of deep-  
567 rooted trees is kept relatively high (Figure 4b) and the trees operate at the upper end of their  
568 vulnerability curve through the year, with typical loss of conductivity < 10% (Fig 7). Therefore,  
569 we don't see much effect of the stomatal strategy on GPP and transpiration in a wet year. At the  
570 upper end of the vulnerability curve, stomata are fully open regardless of the stomatal strategy  
571 (either to be safe or risky). When the drought began in late 2012, annual rainfall fell below the  
572 total root zone storage, thus the deep storage remained depleted throughout the year. During the  
573 drought, the deep-rooted trees were able to operate at the high end of the vulnerability curve in  
574 the wet season, when the rainfall recharged the surface layer. As the surface layers dry, water



575 potentials then gradually falls to the lower end of the vulnerability curve; consequently the  
576 photosynthesis and transpiration start to drop as the dry season progresses. With risky stomata,  
577 trees can drive the soil moisture a little further down. This is why we see the difference in the  
578 effect on GPP and transpiration between different stomatal strategies during the dry season when  
579 the drought progresses.

580 With shallow roots, trees only use surface soil moisture storage. As a result, the surface  
581 water storage is quickly used up after the wet season, and the root zone water potential drops  
582 near the low end of the vulnerability curve during the dry season. Thus, the shallow-rooted trees  
583 operate along the full extent of the vulnerability curve year-round, both during the pre-drought  
584 and drought periods. Therefore, as for the deep-rooted cases, we don't see a strong effect of  
585 stomatal strategy on GPP and transpiration during the wet season, but unlike the deep root cases,  
586 the effect of stomatal strategy on GPP and transpiration during the dry season can be seen  
587 throughout the whole simulation period.

588 Rooting strategies greatly control the spatial pattern of vertical soil water content (Figure  
589 5). With deep roots, the vertical soil moisture variation is more homogeneous due to the  
590 extensive root distribution. With shallow roots, soil becomes extremely dry at the surface (<1m)  
591 and extremely wet in deep layers (>5m) resulting from the aggregated root distribution at upper  
592 layers. Our finding is similar to a recent study conducted by Agee et al. (2021), where the  
593 authors found that the extensive lateral root spreading results in homogeneous soil moisture  
594 distribution. The homogeneous soil moisture pattern may contribute to a more energy efficient  
595 system that reduces plant water stress (Agee et al. 2021) because that minimizes the energy  
596 dissipation loss through water transport (Hildebrandt et al. 2016). Both Agee et al (2021) and our  
597 studies emphasize the importance of the means by which the root distributions determine how  
598 the subsurface storage is utilized.

599 Given the shape of the vulnerability curves, in all these simulations, plants will stop  
600 transpiring when their leaf water potential reaches around -10Mpa with efficient xylem or -  
601 15Mpa with safe xylem, depending on their stomatal strategy (Fig 7). Because we are here  
602 holding the stand structure and leaf area constant to allow comparison between cases, the  
603 simulated leaf water potential of the shallow rooted, risky stomata combination can get as low as  
604 -15Mpa (Figure 4b) during dry seasons even during pre-drought period, which is well below the



605 lowest possible leaf water potential observed (-10Mpa) (Vesala et al., 2017). Leaves will likely  
606 be wilted before the water potential drops below -10Mpa and the tree would have already shed  
607 the leaves due to canopy desiccation. But we specifically do not permit that to occur in these  
608 simulations, so as to keep the different cases comparable. Although it might be unrealistic, the  
609 leaf water potential can serve as an indicate of the degree of canopy desiccation. With no or very  
610 little leaf, trees would rely on the storage carbon to support respiratory demand until the wet  
611 season comes to regrow leaves. Depending on the duration of the dry season, trees may exhaust  
612 the stored carbon and die from carbon starvation. Risky stomata can generate higher GPP (Figure  
613 1a), but also result in longer duration of more negative leaf water potential (Figure 4b). This  
614 suggests that shallow rooted pines at CZ2 with risky stomata will benefit from allocating more  
615 net primary productivity to their storage pools rather than growth in order to reduce the carbon-  
616 starvation mortality. Therefore, even though the model generates unrealistically low leaf water  
617 potentials, the extent and the duration of the simulated very low leaf water potential allows us to  
618 gain some insight on the interaction of plant hydraulic strategy and the life history strategy of  
619 conifer trees under a Mediterranean-type climate.

620 In this simulation, the impacts of xylem traits on GPP and ET are weak and subtle. This is  
621 the result of the relative position of the two vulnerability curves, in particular, the intersection of  
622 the two vulnerability curves in absolute conductivity. When the absolute conductivity is plotted  
623 as a function of pressure (fig. 1b and solid lines in fig. S6), it can be seen that, on the left side of  
624 the intersection, the safe xylem is not only safe but also efficient, and a safety-efficiency tradeoff  
625 of xylem thus only occurs on the right side of the intersection point. Therefore, in shallow-rooted  
626 cases, when the root zone water content—and hence plant water status—is low, safe xylem can  
627 generate slightly higher GPP and ET than unsafe xylem. Furthermore, the two pressure-  
628 conductivity curves diverge mainly at the wet end (corresponding to the wet season). This is  
629 likely because the xylem structures of conifers are very similar, and the range of variation of  
630 xylem traits in the sensitivity analysis are limited to the dominant species at the site. Therefore,  
631 the difference in the xylem traits of conifers do not cause significant impacts on the ecosystem  
632 level fluxes under the Mediterranean-type climate of CZ2, where the ecosystem fluxes are  
633 constrained by energy during the wet season (Goulden et al., 2012). In addition, the maximum  
634 rate of GPP and ET are co-constrained by the stand density, the total leaf area, the maximum  
635 stomatal conductance, and VPD. In this study, we used the static stand structure mode of



636 FATES-Hydro, whereby the stand density and the total leaf biomass (so as total leaf area) of the  
637 trees are held constant. This further limits the effect of xylem traits on GPP and ET.

638

#### 639 4.2 Balancing productivity and mortality risk

640 The hydraulic traits that contribute to high carbon fixation rates often make trees more  
641 susceptible to drought. Stomatal strategy ( $P50_{gs}$ ) can have both positive and negative impact on  
642 the trees, creating a tradeoff in the balance between productivity and physiological stress. The  
643 risky stomata ( $P50_{gs} = P50_x$ ) can generate higher GPP but also result in a greater loss of xylem  
644 conductivity and lower leaf water potential. The tradeoff varies depending on the plant's root  
645 strategy—i.e. having a deep vs. a shallow root distribution—and the moisture state.

646 To better understand the tradeoff between productivity and mortality risk, we plot the  
647 simulated annual average GPP against the fraction of conductivity ( $K/K_{max}$ ) of a 55cm DBH  
648 cohort for two scenarios: deep roots (Fig. 8a) and shallow roots (Fig. 8b), with different  
649 combination of xylem and stomatal strategies. In both scenarios, for each pair of xylem and  
650 stomatal strategies, the GPP per tree increases almost linearly with the  $K/K_{max}$ . But, with  
651 increasing the safety of the stomata, the GPP declines faster with loss of conductivity. This  
652 response is stronger in deep-rooted scenarios. Efficient xylem only slightly increases the  
653 steepness of the lines. The stomatal strategies thus represent points along a gradient of the  
654 tradeoff between growth and mortality risk - the safer the stomata, the more GPP is traded for  
655 reducing the mortality risk.

656 Along this tradeoff space, where trees can maximize their net carbon gains likely depends  
657 on the xylem traits. Studies have shown that trees may temporarily lose xylem conductivity  
658 during mild drought, which can recover once the soil water becomes available. However, under  
659 an extreme drought, their xylem could collapse and permanently damage the xylem conduits. In  
660 this case, trees rely on new sapwood growth to support the transpiration (Brodribb et al. 2010,  
661 Anderegg et al. 2013). At one extreme, if the stomatal behavior is too safe, it will give low GPP  
662 and the tree will be outcompeted for light due to faster-growing neighbors, but at the other  
663 extreme, if the stomata behave very aggressive (risky), it will give high GPP but also empty the  
664 subsurface storage quickly, consequently leading to a prolonged dry period of soil moisture. This



665 would lead to substantial xylem damage (and/or root death), and then the carbon needed to grow  
666 new sapwood (or roots) can exceed the benefit of getting the additional GPP. So, the optimal  
667 location along the gradient would probably be located slightly below the  $K/K_{max}$  associated  
668 with that critical xylem water potential. Currently, the xylem refilling and associated carbon cost  
669 are not incorporated in the FATES-Hydro. These two processes should be implemented in the  
670 model to better understand the water-carbon balance.

671 In the deep-rooted scenario, the values of the pre-drought period and early drought stage  
672 are clustered at the upper-right corner, above  $K/K_{max}$  of 0.6. (Fig. 8a). In this region, the stress  
673 from the loss of xylem conductivity likely won't be high enough to cause severe consequences, if  
674 using 50 percent loss of xylem conductivity as the threshold for mortality and/or permanent  
675 xylem damage. The deep-rooted tree can thus benefit by trading less GPP for maintaining xylem  
676 conductivity with a risky/more-productive stomatal strategy during normal years. But, during the  
677 late stage of the drought (2014 and 2015), the conductivity values become much lower. If this  
678 mega drought stopped earlier, e.g. if it were a mild drought that only lasted for two years, the  
679 additional GPP obtained from risky stomata may outweigh the carbon cost for repairing xylem  
680 damage. This suggests that, if the 2012 – 2015 drought was not common in California, natural  
681 selection might favor the risky/more-productive stomatal strategy for deep-rooted trees.  
682 However, this same strategy also exposes trees to high mortality risk under severe droughts.

683 In the shallow-rooted case (Fig. 8b), the values are all clustered lower and to the left, as  
684 compared to deep rooted scenario, irrespective of the drought status. Thus, for shallow roots,  
685 risky/more-productive stomatal behavior results in a similarly high mortality risk during both the  
686 pre-drought and drought period. Thus, under the long-term climate conditions seen at CZ2,  
687 whether or not severe droughts were frequent, the only shallow-rooted trees that could persist  
688 would have to follow the safe and less-productive stomatal strategy. And, this safe and less-  
689 productive stomata also protects the shallow-rooted tree plant from mortality risk during drought.

690 The model outcome indicates that under drier root zone soil conditions, if pines were to  
691 follow a shallow rooting strategy, they would benefit from a safer stomatal strategy, with more  
692 conservative water use; but if they follow a deep rooting strategy, pines would benefit from  
693 riskier stomata. This is consistent with Anderegg et al.'s (2016) finding on the relative stomatal  
694 conductance ( $g_s$ ) across elevation. They found that at low elevation (lower precipitation) site,





695 Ponderosa pine has lower relative stomatal conductance and less loss of % xylem conductivity,  
696 equivalent to safer stomata in our study, while at mid elevation (higher precipitation) site, pine  
697 has higher relative stomatal conductance and more loss of % xylem conductivity, equivalent to  
698 risky stomata in our study. The simulation results are consistent with the idea that the CZ2 region  
699 is dominated by deep-rooted trees. This is supported by previous studies. In situ measurements of  
700 regolith structure (particular the porosity) indicates that at CZ2, there is a layer of thick semi-  
701 weathered bed rock that allow the trees to grow deep roots (Holbrook et al., 2014). Growing  
702 deep roots to access rock moisture to support plant water use has also been observed in the Eel  
703 River CZO catchment (Rempe et al., 2018), another Mediterranean-type ecosystem along the  
704 west coast. Observed net CO<sub>2</sub> exchange and ET during the pre-drought period suggest that  
705 during a wet year, deep moisture supported summer transpiration and productivity when the  
706 upper layer moisture was low (Goulden et al. 2015). Because the deep rooting strategy is  
707 sufficient in most cases to avoid the main effects of dry seasons and short droughts, and that,  
708 conditional on having deep roots, the risky stomatal strategy confers a productivity advantage at  
709 little increased risk of vulnerability, then we would expect that plants with these traits would  
710 dominate. However, under extreme cases such as the 2012 - 2015 drought, which ranked as one  
711 of the most severe in California in the last 1200 years (Lu et al. 2019), we would expect that  
712 plants with this deep-rooted, risky stomatal strategy would be highly vulnerable to drought,  
713 which is consistent with the ~90% mortality of the pine observed at CZ2 during the drought  
714 (Fettig et al. 2019). The water balance of the catchment based on the long-term observation from  
715 precipitation, stream flow, and ET (Bales et al. 2018, Goulden and Bales 2019) also support that  
716 it was the slow depletion of deep moisture that caused tree mortality in late stage of the  
717 prolonged 2012 – 2015 drought.

718         The finding of our study indicates that the future drought mortality would likely occur in  
719 the ecosystems which are co-limited by water and other factors. In those ecosystems, trees can  
720 benefit from having more efficient but less safe hydraulic traits, which allow them to be more  
721 competitive for water, and bring in higher GPP. The extra carbon gain can be used to develop  
722 measures to deal with other constraining factors, such as increase storage carbon to lower the risk  
723 of carbon starvation, or build thicker bark to resist fire, and to grow more roots which further  
724 enhance their capacity to compete for water.



## 725 5. Conclusions

726 Our analysis indicates that, in a Mediterranean-type climate where the supply of energy  
727 and water is desynchronized and accessible subsurface water storage capacity is close to annual  
728 precipitation, deep roots combined with risky stomata represent a beneficial strategy for high  
729 productivity in normal years, but exposes trees to high mortality risk during multi-year droughts.  
730 While such a strategy enables trees to fully utilize subsurface storage and precipitation for  
731 productivity over the regular years, the lack of deep water storage recharge during droughts  
732 exposes trees to high drought stress and makes this strategy unfavorable under severe and  
733 prolonged drought. In contrast, shallow roots combined with safe stomata represent a strategy for  
734 drought resistance, albeit at the cost of considerably reduced productivity, as such a combination  
735 only allows trees to use shallow subsurface storage while leaving deep moisture untouched, thus  
736 less precipitation is used for productivity. But this strategy leaves trees to be less susceptible to  
737 drought-induced mortality should the deep reservoir be depleted. These results suggest that  
738 stomatal strategy is controlled by root zone soil moisture and regulated by root distribution in  
739 that region. Thus, our study underscores the importance of considering plant rooting and  
740 hydraulic strategies within the larger context of plant ecological strategies.

741

## 742 Author contribution

743 JD and CDK design the study and write the MS. JD conducted the simulation. PB, RB, MG  
744 provided model input data. BC, CDK, RF, RK, CX wrote the code. PB, RB, BC, RF, MG, RK,  
745 LK, JS, CX edited the MS. CDK provided the funding

746

## 747 Acknowledgement

748 We acknowledge support by the Director, Office of Science, Office of Biological and  
749 Environmental Research of the U. S. Department of Energy under Contract DE-AC02-  
750 05CH11231 through the Early Career Research Program, the University of California Laboratory  
751 Fees Research Program, and National Science Foundation Southern Sierra Critical Zone  
752 Observatory grant EAR-1331931.

## 753 Data availability statement

754 The FATES code (branch FATEScodeforMS1), parameter files and data that support the  
755 findings of this study are openly available at ZENODO:  
756 <https://zenodo.org/account/settings/github/repository/JunyanDing/Rooting-and-Hydraulic->



757 [strategy-of-pine-at-Sierra-CZ2-](#) (DOI 10.5281/zenodo.5504405). The flux tower data can be  
758 retrieved from the UC Merced online database (<https://www.ess.uci.edu/~california/>).

759 **Competing interests**

760 The authors declare no conflict of interest



## 761 5. References

- 762 Abatzoglou J.T. and Brown T.J. “A comparison of statistical downscaling methods suited for  
763 wildfire applications” *International Journal of Climatology* (2012), 32, 772-780. 2012.
- 764 Adams, H. D. et al. “Mechanisms in Drought-Induced Tree Mortality.” *Nature Ecology &*  
765 *Evolution* 1(September). <http://dx.doi.org/10.1038/s41559-017-0248-x>. 2017.
- 766 Agee, E., He, L., Bisht, G., Couvreur, V., Shahbaz, P., Meunier, F. et al., 2021. Root lateral  
767 interactions drive water uptake patterns under water limitation. *Adv. Water Resour.*, 151:  
768 103896.
- 769 Anderegg, W.R., Plavcová, L., Anderegg, L.D., Hacke, U.G., Berry, J.A. and Field, C.B.,  
770 Drought's legacy: multiyear hydraulic deterioration underlies widespread aspen forest die-  
771 off and portends increased future risk. *Global change biology*, 19(4), pp.1188-1196. 2013.
- 772 Anderegg, L. D. L. and Hillerislambers, J. Drought stress limits the geographic ranges of two  
773 tree species via different physiological mechanisms *Glob. Chang. Biol.* 22 1029–45  
774 Online: <http://dx.doi.org/10.1111/gcb.13148>. 2016
- 775 Ando, Eigo, and Kinoshita, Toshinori. “Red Light-Induced Phosphorylation of Plasma  
776 Membrane H<sup>+</sup>-ATPase in Stomatal Guard Cells.” *Plant Physiology* 178(October): 838–49.  
777 2018.
- 778 Baker, Kathryn V., Tai, Xiaonan, Miller, Megan L, Johnson, D. M., Six co-occurring conifer  
779 species in northern Idaho exhibit a continuum of hydraulic strategies during an extreme  
780 drought year, *AoB PLANTS*, Volume 11, Issue 5, October 2019, plz056,
- 781 Bales, Roger et al. “Spatially Distributed Water-Balance and Meteorological Data from the Rain  
782 – Snow Transition , Southern Sierra Nevada , California.” : 1795–1805. 2018.
- 783 Bales, Roger et al. 2018. “Mechanisms Controlling the Impact of Multi-Year Drought on  
784 Mountain Hydrology.” *Scientific Reports* (December 2017): 1–8.
- 785 Ball, J. Timothy, Ian E. Woodrow, and Joseph A. Berry. "A model predicting stomatal  
786 conductance and its contribution to the control of photosynthesis under different  
787 environmental conditions." *Progress in photosynthesis research*. Springer, Dordrecht, 221-  
788 224. 1987.
- 789 Barnard, DM, Meinzer, FC, Lachenbruch, B., McCulloh, KA, Johnson, DM, Woodruff, D.R.  
790 Climate-related trends in sapwood biophysical properties in two conifers: avoidance of  
791 hydraulic dysfunction through coordinated adjustments in xylem efficiency, safety and  
792 capacitance. *Plant Cell Environ.* Apr;34(4):643-54. doi: 10.1111/j.1365-3040.2010.02269.x.  
793 Epub 2011 Feb 11. PMID: 21309793. 2011
- 794 Bartlett, M.K., Klein, T., Jansen, S., Choat, B. and Sack, L., The correlations and sequence of  
795 plant stomatal, hydraulic, and wilting responses to drought. *Proceedings of the National*  
796 *Academy of Sciences*, 113(46), pp.13098-13103. 2016.
- 797 Brodribb, T.J., Bowman, D.J., Nichols, S., Delzon, S. and Burtlett, R., 2010. Xylem function and  
798 growth rate interact to determine recovery rates after exposure to extreme water deficit.  
799 *New Phytologist*, 188(2), pp.533-542.



- 800 Buotte, Polly C., Samuel Levis, Beverly E. Law, Tara W. Hudiburg, David E. Rupp, and Jeffery  
801 J. Kent. “Near - Future Forest Vulnerability to Drought and Fire Varies across the Western  
802 United States.” (July):1–14. 2018.
- 803 Canadell, J.G., Le Quéré, C., Raupach, M.R., Field, C.B., Buitenhuis, E.T., Ciais, P., Conway,  
804 T.J., Gillett, N.P., Houghton, R.A. and Marland, G., Contributions to accelerating  
805 atmospheric CO<sub>2</sub> growth from economic activity, carbon intensity, and efficiency of natural  
806 sinks. *Proceedings of the national academy of sciences*, 104(47), pp.18866-18870. 2007.
- 807 Choat, Brendan, and Jarmila Pittermann. “New Insights into Bordered Pit Structure and  
808 Cavitation Resistance in Angiosperms and Conifers.” *New Phytologist*: 555–57. 2009.
- 809 Christoffersen, B. O. et al. “Linking Hydraulic Traits to Tropical Forest Function in a Size-  
810 Structured and Trait-Driven Model (TFS v. 1-Hydro ).” : 4227–55. 2016.
- 811 Coley, P.D., Bryant, J.P. and Chapin, F.S., Resource availability and plant antiherbivore  
812 defense. *Science*, 230(4728), pp.895-899. 1985.
- 813 Corcuera, L., Cochard, H., Gil-Pelegrin, E. and Notivol, E., Phenotypic plasticity in mesic  
814 populations of *Pinus pinaster* improves resistance to xylem embolism (P 50) under severe  
815 drought. *Trees*, 25(6), pp.1033-1042. 2011.
- 816 Craine, J.M., Tilman, D., Wedin, D., Reich, P., Tjoelker, M. and Knops, J., Functional traits,  
817 productivity and effects on nitrogen cycling of 33 grassland species. *Functional  
818 Ecology*, 16(5), pp.563-574. 2002.
- 819 Danabasoglu, G. et al. “The Community Earth System Model Version 2 ( CESM2 ) Journal of  
820 Advances in Modeling Earth Systems.” *Journal of Advances in Modeling Earth Systems* 2:  
821 1–35. 2020.
- 822 Domec, J.C., Warren, J.M., Meinzer, F.C. et al. Native root xylem embolism and stomatal closure  
823 in stands of Douglas-fir and ponderosa pine: mitigation by hydraulic  
824 redistribution. *Oecologia* **141**, 7–16 <https://doi.org/10.1007/s00442-004-1621-4>. 2004.
- 825 Fettig, Christopher J, Leif A Mortenson, M Bu, and Patra B Fou. “Tree Mortality Following  
826 Drought in the Central and Southern Sierra Nevada, California, U.S.” *Forest Ecology and  
827 Management* 432: 164–78. 2019.
- 828 Fisher, R. a. et al. “Taking off the Training Wheels: The Properties of a Dynamic Vegetation  
829 Model without Climate Envelopes, CLM4.5(ED).” *Geoscientific Model Development* 8(11):  
830 3593–3619. 2015.
- 831 Gaylord, M.L., Kolb, T.E. and McDowell, N.G.,. Mechanisms of piñon pine mortality after  
832 severe drought: a retrospective study of mature trees. *Tree physiology*, 35(8), pp.806-816.  
833 2015
- 834 Geen, Anthony Toby O et al. “Southern Sierra Critical Zone Observatory and Kings River  
835 Experimental Watersheds : A Synthesis of Measurements , New Insights , and Future  
836 Directions.” *Vadose Zone J. Advancing Critical Zone Science* Advancing Critical Zone  
837 Science. 2018.
- 838 Gleason, Sean M., Mark Westoby, Steven Jansen, Brendan Choat, Uwe G. Hacke, Robert B.



- 839 Pratt, Radika Bhaskar, Tim J. Brodribb, Sandra J. Bucci, Kun Fang Cao, Hervé Cochard,  
840 Sylvain Delzon, Jean Christophe Domec, Ze Xin Fan, Taylor S. Feild, Anna L. Jacobsen,  
841 Daniel M. Johnson, Frederic Lens, Hafiz Maherali, Jordi Martínez-Vilalta, Stefan Mayr,  
842 Katherine A. Mcculloh, Maurizio Mencuccini, Patrick J. Mitchell, Hugh Morris, Andrea  
843 Nardini, Jarmila Pittermann, Lenka Plavcová, Stefan G. Schreiber, John S. Sperry, Ian J.  
844 Wright, and Amy E. Zanne. “Weak Tradeoff between Xylem Safety and Xylem-Specific  
845 Hydraulic Efficiency across the World’s Woody Plant Species.” *New Phytologist*  
846 209(1):123–36. 2016.
- 847 Golaz, Jean-Christophe, Luke P. Van Roekel, Xue Zheng, Andrew F. Roberts, Jonathan D.  
848 Wolfe, Wuyin Lin, Andrew M. Bradley et al. "The DOE E3SM Model Version 2: overview  
849 of the physical model and initial model evaluation." *Journal of Advances in Modeling Earth*  
850 *Systems* 14, no. 12 (2022).
- 851 Goulden, M L et al. “Evapotranspiration along an Elevation Gradient in California ’ s Sierra  
852 Nevada.” *Journal of Geophysical Research* 117(1): 1–13. 2015.
- 853 Goulden, M L, and R C Bales. 2019. “California Forest Die-off Linked to Multi-Year Deep Soil  
854 Drying in 2012–2015 Drought.” *Nature Geoscience* 12(August).  
855 <http://dx.doi.org/10.1038/s41561-019-0388-5>.
- 856 Grime, J.P., Evidence for the existence of three primary strategies in plants and its relevance to  
857 ecological and evolutionary theory. *The American Naturalist*, 111(982), pp.1169-1194.  
858 1977.
- 859 Grime, J.P., Plant strategies and vegetation processes. *Plant strategies and vegetation processes*.  
860 1979.
- 861 Hacke, Uwe G., Rachel Spicer, Stefan G. Schreiber, and Lenka Plavcová. “An Ecophysiological  
862 and Developmental Perspective on Variation in Vessel Diameter.” *Plant Cell and*  
863 *Environment* 40(6):831–45. 2017.
- 864 Hammond, W., K. Yu<sup>+</sup>, L. Wilson, R. Will, W.R.L. Anderegg, and H. Adams. 2019. “Dead or  
865 dying? Quantifying the point of no return from hydraulic failure in drought-induced tree  
866 mortality”. *New Phytologist*. doi: 10.1111/nph.15922. Published, 05/2019
- 867 Hartmann, Henrik, Waldemar Ziegler, Olaf Kolle, and Susan Trumbore. “Thirst Beats Hunger -  
868 Declining Hydration during Drought Prevents Carbon Starvation in Norway Spruce  
869 Saplings.” *New Phytologist* 200(2):340–49. 2013.
- 870 Hartung, Wolfram, Angela Sauter, and Eleonore Hose. “Abscisic Acid in the Xylem : Where  
871 Does It Come from , Where Does It Go To ?” *Plant Physiology* 53(366): 27–32. 2002.
- 872 Hetherington, Alistair M, and F Ian Woodward. “The Role of Stomata in Sensing and Driving  
873 Environmental Change.” *Nature* 424(August): 901–8. 2003.
- 874 Huang, J., Kautz, M., Trowbridge, A. M., Hammerbacher, A., Raffa, K. F., Adams, H. D., ... &  
875 Gershenson, J. Tree defence and bark beetles in a drying world: carbon partitioning,  
876 functioning and modelling. *New Phytologist*, 225(1), 26-36. (2020).
- 877 Inouea, Shin-ichiro, and Toshinori Kinoshitaa. 2017. “Blue Light Regulation of Stomatal  
878 Opening and the Plasma Membrane H<sup>+</sup>-ATPase 2.” *Plant Physiology* (166): 17.



- 879 Ivanov, Valeriy Y., Lucy R. Hutyra, Steven C. Wofsy, J. William Munger, Scott R. Saleska,  
880 Raimundo C. De Oliveira, and Plínio B. De Camargo. “Root Niche Separation Can Explain  
881 Avoidance of Seasonal Drought Stress and Vulnerability of Overstory Trees to Extended  
882 Drought in a Mature Amazonian Forest.” *Water Resources Research* 48(12):1–21. 2012.
- 883 Jackson, R.B., Canadell, J., Ehleringer, J.R., Mooney, H.A., Sala, O.E. and Schulze, E.D., A  
884 global analysis of root distributions for terrestrial biomes. *Oecologia*, 108(3), pp.389-411.  
885 1996.
- 886 Johnson, D. M., Domec, J. C., Carter Berry, Z., Schwantes, A. M., McCulloh, K. A., Woodruff,  
887 D. R., ... & McDowell, N. G. Co-occurring woody species have diverse hydraulic strategies  
888 and mortality rates during an extreme drought. *Plant, Cell & Environment*, 41(3), 576-588.  
889 2018.
- 890 Kattge, J., Bönisch, G., Díaz, S., Lavorel, S., Prentice, I. C., Leadley, P., Tautenhahn, S., Werner,  
891 G., et al. “TRY Plant Trait Database - Enhanced Coverage and Open Access.” *Global  
892 Change Biology* 26(1):119–88. 2020.
- 893 Kelly, Anne E, and Michael L Goulden. “A Montane Mediterranean Climate Supports Year-  
894 Round Photosynthesis and High Forest Biomass.” : 459–68. 2016.
- 895 Khasanova, Albina, John T. Lovell, Jason Bonnette, Xiaoyu Weng, Jerry Jenkins, Yuko  
896 Yoshinaga, Jeremy Schmutz, and Thomas E. Juenger. “The Genetic Architecture of Shoot  
897 and Root Trait Divergence between Mesic and Xeric Ecotypes of a Perennial Grass.”  
898 *Frontiers in Plant Science* 10(April):1–10. 2019.
- 899 Kilgore, J.S., Jacobsen, A.L. and Telewski, F.W., Hydraulics of Pinus (subsection Ponderosae)  
900 populations across an elevation gradient in the Santa Catalina Mountains of southern  
901 Arizona. *Madroño*, 67(4), pp.218-226. 2021.
- 902 Klos, P Zion et al. “Subsurface Plant-Accessible Water in Mountain Ecosystems with a  
903 Mediterranean Climate.” *Wiley Interdisciplinary Reviews: Water* (May 2017): 1–14. 2017.
- 904 Koch, G.W. and Fredeen, A.L., Transport challenges in tall trees. In *Vascular transport in  
905 plants* (pp. 437-456). Academic Press. 2005.
- 906 Koven, C.D., Knox, R.G., Fisher, R.A., Chambers, J.Q., Christoffersen, B.O., Davies, S.J.,  
907 Detto, M., Dietze, M.C., Faybishenko, B., Holm, J. and Huang, M., Benchmarking and  
908 parameter sensitivity of physiological and vegetation dynamics using the Functionally  
909 Assembled Terrestrial Ecosystem Simulator (FATES) at Barro Colorado Island,  
910 Panama. *Biogeosciences*, 17(11), pp.3017-3044. 2020.
- 911 Kulmatiski, Andrew and Karen H. Beard. “Root Niche Partitioning among Grasses, Saplings,  
912 and Trees Measured Using a Tracer Technique.” *Oecologia* 171(1):25–37. 2013.
- 913 Lawrence, D.M., Fisher, R.A., Koven, C.D., Oleson, K.W., Swenson, S.C., Bonan, G., Collier,  
914 N., Ghimire, B., van Kampenhout, L., Kennedy, D. and Kluzek, E., The Community Land  
915 Model version 5: Description of new features, benchmarking, and impact of forcing  
916 uncertainty. *Journal of Advances in Modeling Earth Systems*, 11(12), pp.4245-4287.
- 917 Li, S., Lens, F., Espino, S., Karimi, Z., Klepsch, M., Schenk, H.J., Schmitt, M., Schuldt, B. and



- 1918 Jansen, S., 2016. Intervessel pit membrane thickness as a key determinant of embolism  
1919 resistance in angiosperm xylem. *Iawa Journal*, 37(2), pp.152-171. 2019.
- 1920 Lu, Yaojie et al. 2019. “Optimal Stomatal Drought Response Shaped by Competition for Water  
1921 and Hydraulic Risk Can Explain Plant Trait Covariation.” (1977).
- 1922 Mackay, D. S., Savoy, P. R., Grossiord, C., Tai, X., Pleban, J. R., Wang, D. R., ... & Sperry, J. S.  
1923 Conifers depend on established roots during drought: results from a coupled model of  
1924 carbon allocation and hydraulics. *New Phytologist*, 225(2), 679-692. 2020.
- 1925 Martínez-Vilalta, Jordi, Anna Sala, and Josep Piñol. *The Hydraulic Architecture of Pinaceae-a*  
1926 *Review*. Vol. 171. 2004.
- 1927 Matheny, Ashley M, Golnazalsadat Mirfenderesgi, and Gil Bohrer. “Trait-Based Representation  
1928 of Hydrological Functional Properties of Plants in Weather and Ecosystem Models.” *Plant*  
1929 *Diversity* 39(1): 1–12. <http://dx.doi.org/10.1016/j.pld.2016.10.001>. 2017.
- 1930 Matheny, A.M., Fiorella, R.P., Bohrer, G., Poulsen, C.J., Morin, T.H., Wunderlich, A., Vogel,  
1931 C.S. and Curtis, P.S., Contrasting strategies of hydraulic control in two codominant  
1932 temperate tree species. *Ecohydrology*, 10(3), p.e1815. 2017.
- 1933 Mcdowell, Nate, Nate Mcdowell, William T. Pockman, Craig D. Allen, D. David, Neil Cobb,  
1934 Thomas Kolb, Jennifer Plaut, John Sperry, Adam West, David G. Williams, and Enrico A.  
1935 Yepez. “Mechanisms of Plant Survival and Mortality during Drought : Why Do Some  
1936 Plants Survive While Others Succumb To.” 2008.
- 1937 McDowell, Nate G. et al. “Evaluating Theories of Drought-Induced Vegetation Mortality Using  
1938 a Multimodel – Experiment Framework.” : 304–21. 2013.
- 1939 Mooney, Harold and Erika Zavaleta. *Ecosystems of California*. Vol. 3. edited by H. Mooney and  
1940 E. Zavaleta. Oakland, California, USA: Univ of California Press. 2003.
- 1941 Mursinna, A. Rio, Erica McCormick, Kati Van Horn, Lisa Sartin, and Ashley M. Matheny.  
1942 “Plant Hydraulic Trait Covariation: A Global Meta-Analysis to Reduce Degrees of Freedom  
1943 in Trait-Based Hydrologic Models.” *Forests* 9(8). 2018.
- 1944 Oleson, Keith W et al. “Technical Description of Version 4.5 of the Community Land Model  
1945 (CLM) Coordinating.” In *Natl. Cent. Atmos. Res. Tech. Note*, Natl. Cent. for Atmos. Res.,  
1946 Boulder, Colo. 2013.
- 1947 Pittermann, Jarmila, John S. Sperry, Uwe G. Hacke, James K. Wheeler, and Elzard H. Sikkema.  
1948 “Inter-Tracheid Pitting and the Hydraulic Efficiency of Conifer Wood: The Role of  
1949 Tracheid Allometry and Cavitation Protection.” *American Journal of Botany* 93(9):1265–  
1950 73. 2006.
- 1951 Pittermann, Jarmila, John S. Sperry, James K. Wheeler, Uwe G. Hacke, and Elzard H. Sikkema.  
1952 “Mechanical Reinforcement of Tracheids Compromises the Hydraulic Efficiency of Conifer  
1953 Xylem.” *Plant, Cell and Environment* 29(8):1618–28. 2006.
- 1954 Pockman, W.T. and Sperry, J.S., Vulnerability to xylem cavitation and the distribution of  
1955 Sonoran desert vegetation. *American journal of botany*, 87(9), pp.1287-1299. 2000.





- 956 Powell, Thomas L., James K. Wheeler, Alex A. R. de Oliveira, Antonio Carlos Lola da Costa,  
957 Scott R. Saleska, Patrick Meir, and Paul R. Moorcroft. "Differences in Xylem and Leaf  
958 Hydraulic Traits Explain Differences in Drought Tolerance among Mature Amazon  
959 Rainforest Trees." *Global Change Biology* 23(10):4280–93. 2017.
- 960 Pratt, R.B. and Jacobsen, A.L., Conflicting demands on angiosperm xylem: tradeoffs among  
961 storage, transport and biomechanics. *Plant, Cell & Environment*, 40(6), pp.897-913. 2017.
- 962 Reich, Peter B., Ian J. Wright, Jeannine Cavender-Bares, J. M. Craine, Jacek Oleksyn, M.  
963 Westoby, and M. B. Walters. "The evolution of plant functional variation: traits, spectra,  
964 and strategies." *International Journal of Plant Sciences* 164, no. S3: S143-S164. (2003).
- 965 Reichstein, M., Bahn, M., Mahecha, M.D., Kattge, J. and Baldocchi, D.D., Linking plant and  
966 ecosystem functional biogeography. *Proceedings of the National Academy of  
967 Sciences*, 111(38), pp.13697-13702. 2014.
- 968 Rodriguez-Dominguez, C.M., Buckley, T.N., Egea, G., de Cires, A., Hernandez-Santana, V.,  
969 Martorell, S. and Diaz-Espejo, A., Most stomatal closure in woody species under moderate  
970 drought can be explained by stomatal responses to leaf turgor. *Plant, Cell &  
971 Environment*, 39(9), pp.2014-2026. 2016.
- 972 Rowland, L., A. C. L. Da Costa, D. R. Galbraith, R. S. Oliveira, O. J. Binks, A. A. R. Oliveira,  
973 A. M. Pullen, C. E. Doughty, D. B. Metcalfe, S. S. Vasconcelos, L. V. Ferreira, Y. Malhi, J.  
974 Grace, M. Mencuccini, and P. Meir. "Death from Drought in Tropical Forests Is Triggered  
975 by Hydraulics Not Carbon Starvation." *Nature* 528(7580):119–22. 2015.
- 976 Salmon, Yann, José M. Torres-Ruiz, Rafael Poyatos, Jordi Martinez-Vilalta, Patrick Meir, Hervé  
977 Cochard, and Maurizio Mencuccini. "Balancing the Risks of Hydraulic Failure and Carbon  
978 Starvation: A Twig Scale Analysis in Declining Scots Pine." *Plant Cell and Environment*  
979 38(12):2575–88. 2015.
- 980 Sauter, Angela, W J Davies, Wolfram Hartung, and Lehrstuhl Botanik I. "The Long-Distance  
981 Abscisic Acid Signal in the Droughted Plant : The Fate of the Hormone on Its Way from  
982 Root to Shoot." 52(363): 1991–97. 2001.
- 983 Skelton, R. P., West, A. G., & Dawson, T. E. "Predicting plant vulnerability to drought in  
984 biodiverse regions using functional traits." *Proceedings of the National Academy of  
985 Sciences*, 112(18), 5744-5749. 2015.
- 986 Sevanto, Sanna, Nate G. McDowell, L. Turin Dickman, Robert Pangle, and William T. Pockman.  
987 "How Do Trees Die? A Test of the Hydraulic Failure and Carbon Starvation Hypotheses."  
988 *Plant, Cell and Environment* 37(1):153–61. 2014.
- 989 Sperry, John S. "Evolution of Water Transport and Xylem Structure." *International Journal of  
990 Plant Sciences* 164. 2003.
- 991 Teuling, Adriaan J, Remko Uijlenhoet, and Peter A Troch. "Impact of Plant Water Uptake  
992 Strategy on Soil Moisture and Evapotranspiration Dynamics during Drydown." 33: 3–7.  
993 2006.
- 994 Vesala, T., Sevanto, S., Grönholm, T., Salmon, Y., Nikinmaa, E., Hari, P. and Hölttä, T., Effect



- 995 of leaf water potential on internal humidity and CO<sub>2</sub> dissolution: reverse transpiration and  
996 improved water use efficiency under negative pressure. *Frontiers in plant science*, 8, p.54.  
997 2017.
- 998 Westoby, M., Falster, D.S., Moles, A.T., Vesk, P.A. and Wright, I.J., Plant ecological strategies:  
999 some leading dimensions of variation between species. *Annual review of ecology and*  
1000 *systematics*, 33(1), pp.125-159. 2002.
- 1001 Wilkinson, S, and W J Davies. “ABA-Based Chemical Signalling : The Co-Ordination Of.” :  
1002 195–210. 2002.
- 1003 Wullschleger, Stan D. et al. “Plant Functional Types in Earth System Models : Past Experiences  
1004 and Future Directions for Application of Dynamic Vegetation Models in High-Latitude  
1005 Ecosystems.” *Annals of botany* (114): 1–16. 2014.
- 1006 Yu, Gui-ruì, Jie Zhuang, and Keiichi Nakayama. “Root Water Uptake and Profile Soil Water  
1007 as Affected by Vertical Root Distribution.” *Plant Ecol*: 15–30. 2007.
- 1008 Zeng, Xubin. “Global Vegetation Root Distribution for Land Modeling.” *Journal of*  
1009 *Hydrometeorology* 2(5): 525–30. 2001.
- 1010
- 1011



1012 **Tables**

1013 **Table 1 Parameters used in FATES-Hydro sensitivity analysis**

1014

Parameters	Biological meaning	Values	Units
$r_a, r_b$	Root distribution: shallow roots vs. deep roots	(0.1, 0.1) – (2 5)	unitless
$P50_{gs}$	Leaf xylem water potential at half stomatal closure stomatal control on safety vs. efficiency	$P50_x - P20_x$	Mpa
$P50_x$	Xylem water potential when xylem loss half of the conductance	-3.0 <sup>a</sup> , -4.8 <sup>b</sup>	Mpa
$K_{max}$	Maximum xylem conductivity per unit sap area	0.88 <sup>a</sup> , 0.64 <sup>b</sup>	kg/MPa/m/s
A	Shape parameter of van Genuchten hydrologic function	0.11855 <sup>a</sup> , 0.088026 <sup>b</sup>	Mpa <sup>-1</sup>
m, n	Shape parameters of van Genuchten hydrologic function	(0.8, 1.25) <sup>a</sup> , (0.8, 1.5) <sup>b</sup>	unitless

1015 a: values for efficient/unsafe xylem

1016 b: values for inefficient/safe xylem

1017



Table 2. List of major parameters

Symbol	Source code name	Value	Units	Description	Source
$a_{gs}$	fates_hydr_avuln_gs	2.5	unitless	shape parameter for stomatal control of water vapor (slope) exiting leaf	Christoffersen et al., 2016
$\chi$	fates_hydr_p_taper	0.333	unitless	xylem taper exponent	Christoffersen et al., 2016
$\pi_{o,l}, \pi_{o,s}, \pi_{o,r}$	fates_hydr_pinot_node	-1.47, -1.23, -1.04	MPa	osmotic potential at full turgor of leaf, stem, root	Christoffersen et al., 2016
$RWC_{res,l}, RWC_{res,s}, RWC_{res,r}$	fates_hydr_resid_node	0.25, 0.325, 0.15	proportion	residual fraction of leaf, stem, root	Christoffersen et al., 2016
$\Theta_{sat,x}$	fates_hydr_thetas_node	0.65	cm <sup>3</sup> /cm <sup>3</sup>	saturated water content of xylem	Christoffersen et al., 2016
$SLA_{max}$	fates_leaf_slamax	0.01	m <sup>2</sup> /gC	Maximum Specific Leaf Area (SLA)	TRY
$SLA_{top}$	fates_leaf_slatop	0.01	m <sup>2</sup> /gC	Specific Leaf Area (SLA) at top of canopy, projected area basis	TRY
$V_{cmax,25,top}$	fates_leaf_vcmax25top	55	umol CO <sub>2</sub> /m <sup>2</sup> /s	maximum carboxylation rate of Rub. at 25C, canopy top	TRY
$b_{opt}$	fates_bbopt_c3	10000	umol H <sub>2</sub> O/m <sup>2</sup> /s	Ball-Berry minimum leaf stomatal conductance for C3 plants	Calibrated



## Figures

Figure 1

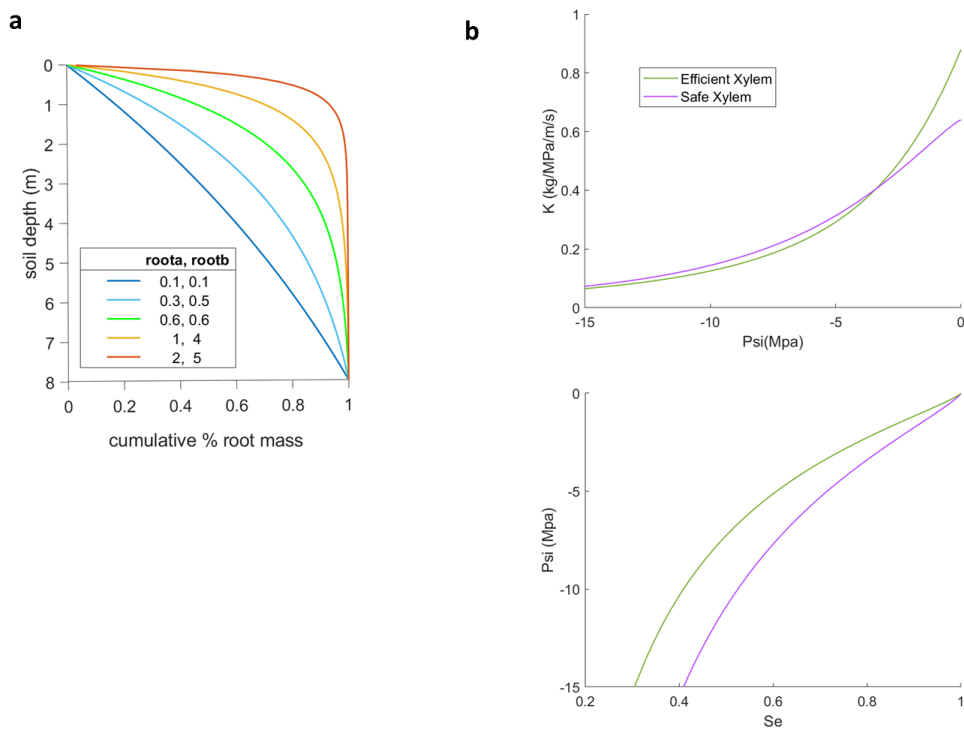


Figure 1. Sensitivity analysis set up for: a) root parameters that give five root distribution scenarios with effective rooting depths of 1m, 3m, 5m, 6.5m, and 8m, and b) two xylem scenarios for safe xylem ( $P50x=-4.8$ ,  $K_{max}=0.64$ ), and efficient xylem ( $P50x=-2.5$ ,  $K_{max}=0.88$ ).



Figure 2

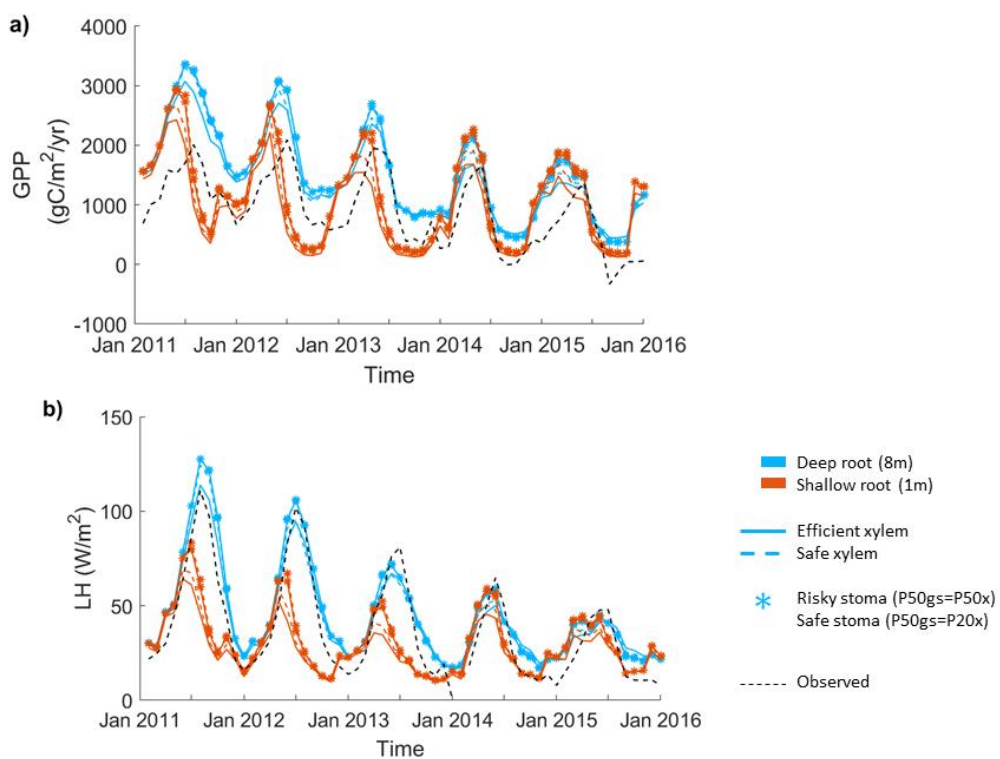


Figure 2. Impact of hydraulic strategies on ecosystem water and energy fluxes: a) monthly mean gross primary productivity, and B) monthly mean latent heat flux, of the end member cases.



Figure 3

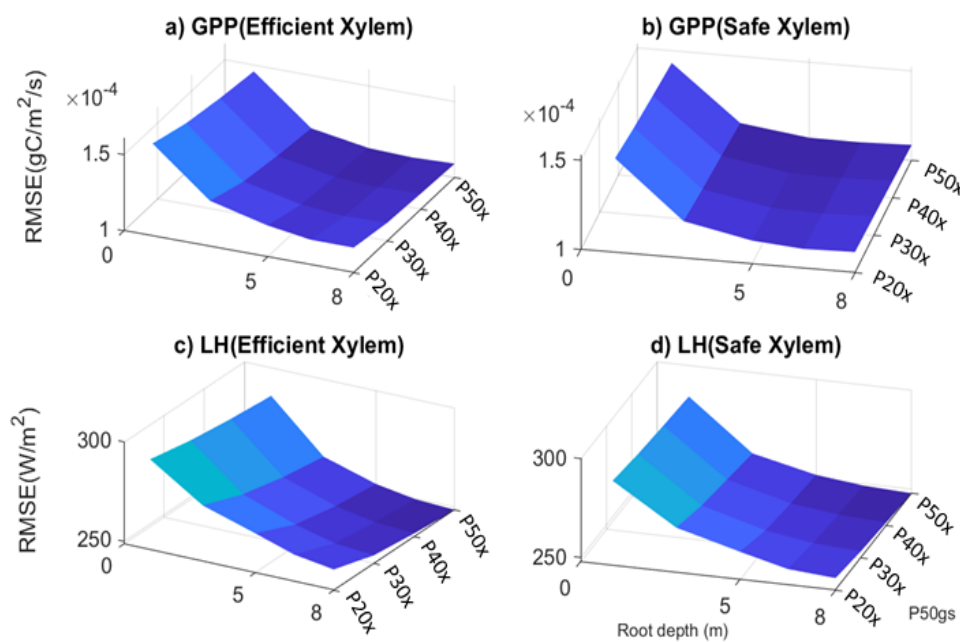


Figure 3. Root mean square error of GPP (a-b), and latent heat flux (c-d) with respect to variation in input parameters.



Figure 4

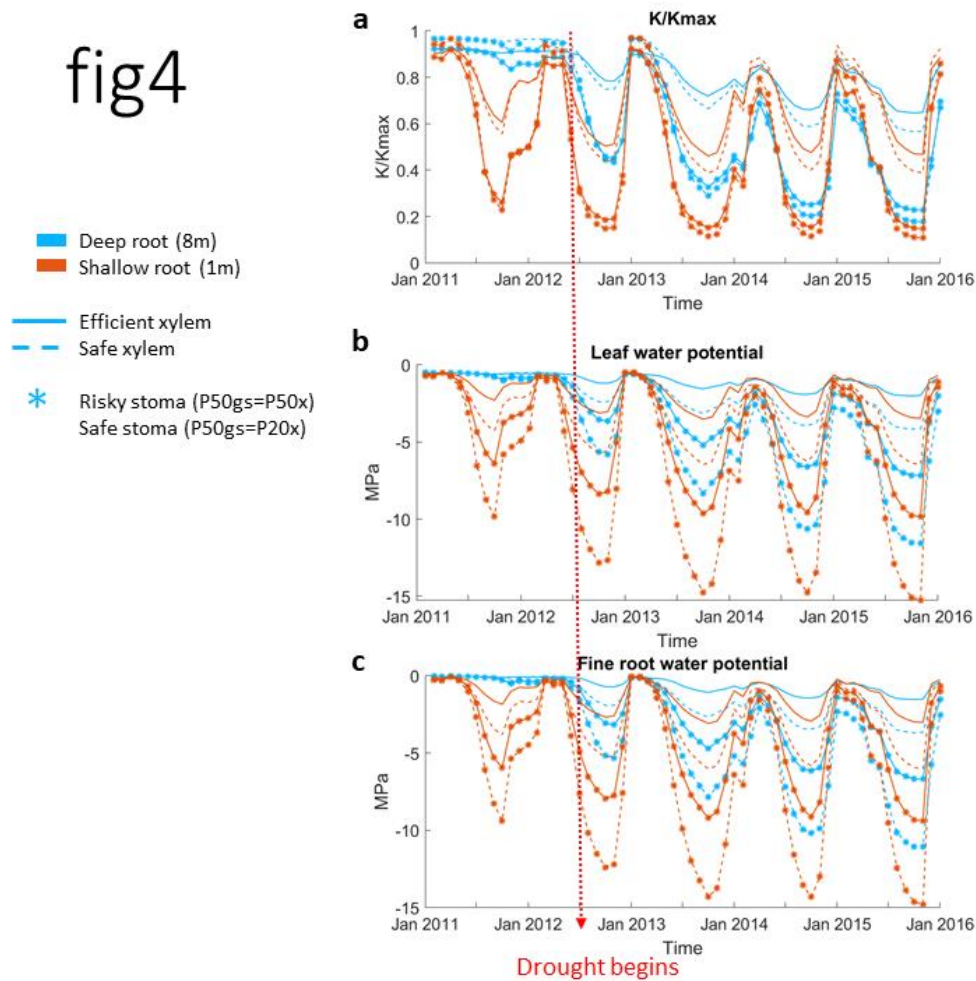


Figure 4. Seasonal and inter-annual variation of plant physiologic characteristics: a) monthly mean stem fraction of conductance  $K/K_{max}$  (a), monthly mean leaf water potential, and c) monthly mean overall absorbing roots water potential, of the 55cm DBH cohort throughout the 2011-2015 period.





Figure 5

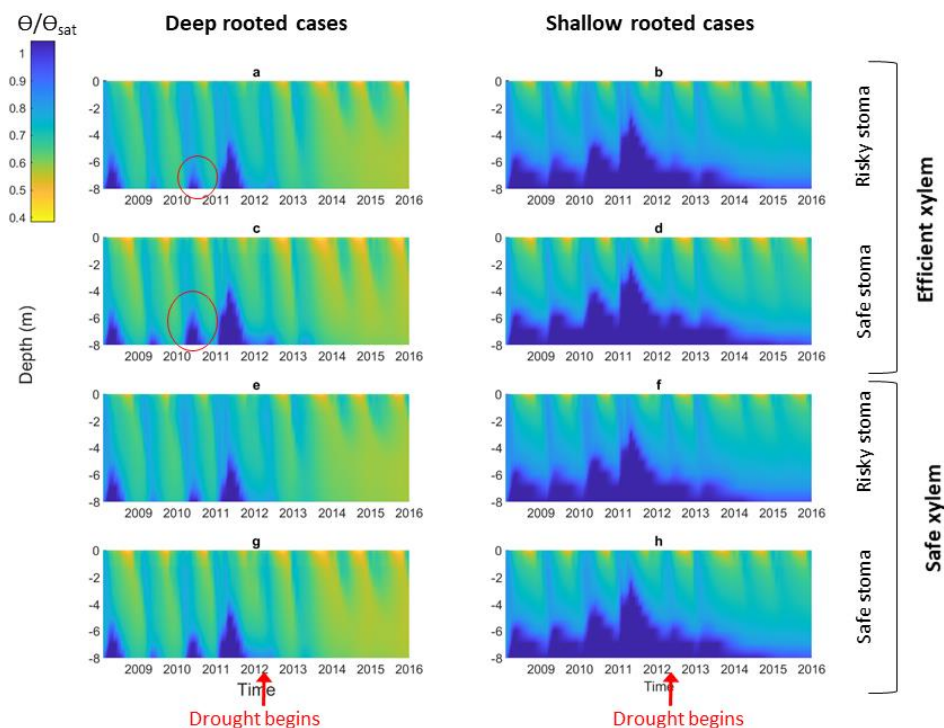


Figure 5. Impact of different combination of rooting depth, xylem and stomatal traits on soil moisture; left column shows deep rooted cases with a) efficient xylem and risky stoma, c) efficient xylem and safe stoma, e) safe xylem and risky stoma, g) safe xylem and safe stoma. Right column shows shallow rooted cases with b) efficient xylem and risky stoma, d) efficient xylem and safe stoma, f) safe xylem and risky stoma, h) safe xylem and safe stoma; red cycle highlights the effect of stomatal traits on deep water storage during the wet season of the pre-drought period



Figure 6

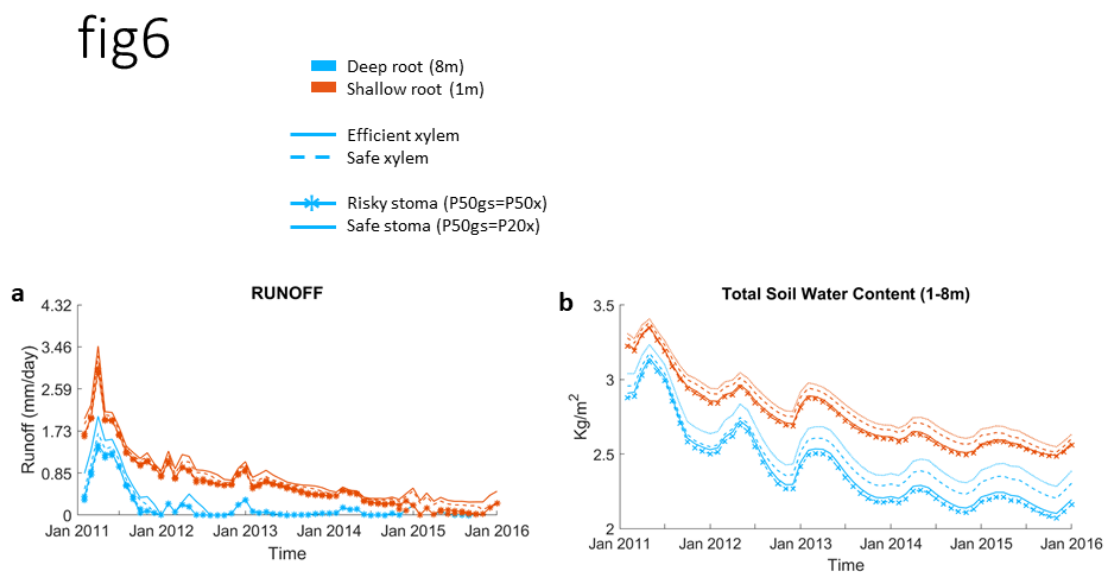


Figure 6. Impact on hydrologic processes: a) mean monthly total runoff, and b) monthly mean total soil water content of the entire soil column.



Figure 7

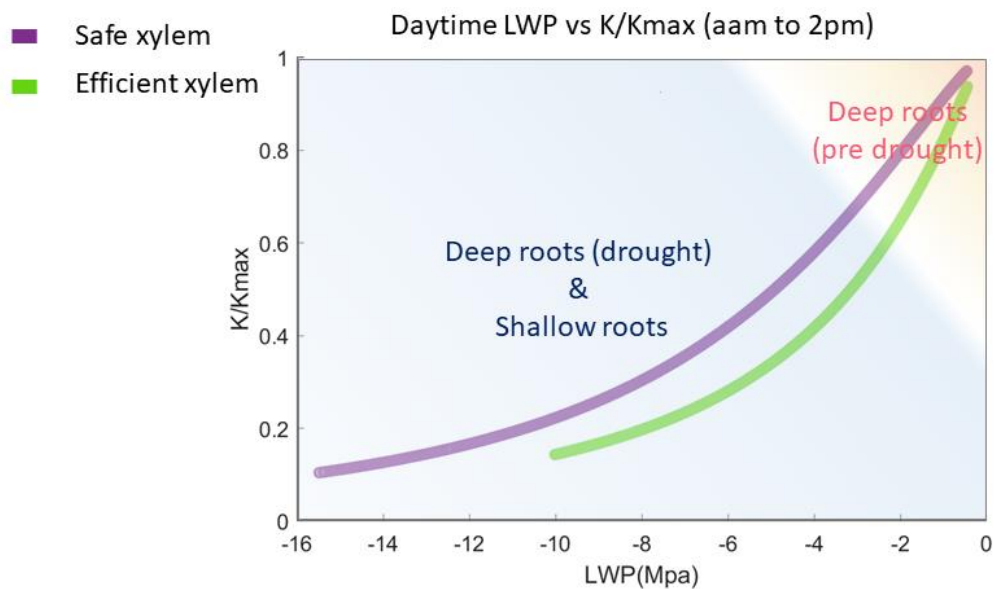


Figure 7. Simulated leaf water potential and fraction loss of conductivity ( $K/K_{max}$ ) of all the cases, which follow the two vulnerability curves.



Figure 8

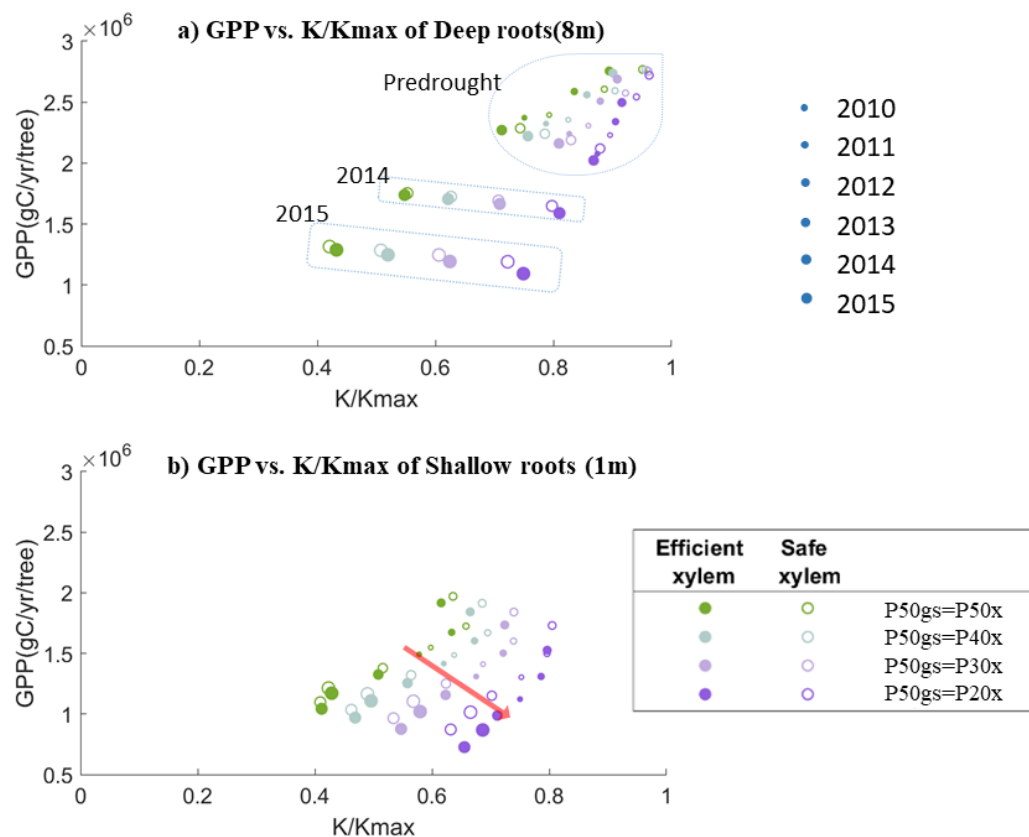


Figure 8. Simulated average annual GPP and fraction of conductance of a 55cm DBH cohort with a) deep roots (effective rooting depth= 8m) and b) shallow roots (effective rooting depth= 1m).